ELSEVIER

Sedimentary Geology 126 (1999) 271–304

Sedimentary Geology

Nature and environmental significance of microbialites in Quaternary reefs: the Tahiti paradox

Gilbert F. Camoin [a,*], Pascale Gautret [b], Lucien F. Montaggioni [c], Guy Cabioch [d]

[a] *CEREGE, C.N.R.S. UMR 6635, B.P. 80, 13545 Aix-en-Provence Cédex 4, France*
[b] *Université Paris 11-Orsay, Laboratoire de Paléontologie, Bâtiment 504, 91405 Orsay Cédex, France*
[c] *C.N.R.S. UPRESA 6019, Université de Provence, 3 Place V. Hugo, 13331 Marseille Cédex 3, France*
[d] *I.R.D. (ex ORSTOM) (Institut de Recherche pour le Développement), Centre de Nouméa, B.P. A5, 98848 Nouméa Cédex, New Caledonia*

Received 12 March 1998; accepted 3 March 1999

Abstract

Drill cores from the barrier reef-edge of Tahiti exhibit 85–93-m-thick coralgal sequences recording at least 13,500 years of continuous reef growth in optimal environmental conditions. The cored reef sequences form an overall shallowing-upward succession with assemblages of branching or massive colonies of *Porites* at the base overlain by a robust-branching community (*Acropora* gr. *danai/robusta*) heavily encrusted by coralline algae, sessile vermetid gastropods and arborescent foraminifers, which grew at depths less than 6 m. Microbialites generally form the last stage of encrustation of coral colonies, or more commonly, of related encrusting organisms, thus appearing as a major structural component of the reef sequence where they may locally form 80% of the rock by volume. They developed in an open cavity system of the reef framework with freely circulating normal-marine water. Microbialites include laminated crusts and clotted micritic masses, commonly associated in compound crusts, probably reflecting differences in the composition of the involved biological communities and in biomineralization processes that controlled the accretion of the crusts. The isotopic composition of the microbialites (+2.05 to +3.92‰ $\delta^{13}C$ and −0.86 to +0.86‰ $\delta^{18}O$) are typical for a non-enzymatic fractionation and are close to those expected for calcitic cements precipitated at equilibrium with normal seawater. The relative scarcity of extraneous particles in the Tahiti crusts suggests that sediment trapping was much less important than calcification of organic mucilage associated with living or decaying organisms, and in-place, microbially mediated, precipitation of micrite. The biochemical composition of the crusts is especially characterized by concentrations of aspartic (Asp) and glutamic (Glu) acids of 10 to 15%: abundant hydroxyproline indicates that metazoans may have proliferated in these microenvironments and represent the first 'donors' of the organic substrates, which may correspond to the mineralizing matrix after recycling by the microbial biofilms. Microbial organisms (especially bacteria and possible nannobacteria) seemingly played a major role in transformation processes and in carbonate precipitation via the bacterial degradation of organic matter; they underwent also individual processes of biomineralization. Besides the overall decrease in light and energy conditions reflecting progressive burial by coral growth, the widespread development of microbialites within the reef framework may be related to increased alkalinity and nutrient availability in interstitial waters due to terrestrial groundwater seepage and periodic runoffs. The development of microbialites in the cryptic niches of the reef framework ceased about 6000 years ago when the sea level approached its present position.

Keywords: microbialites: Holocene; reefs; sea level changes; reef framework; French Polynesia

* Corresponding author. Tel.: +33-442-971-514; Fax: +33-442-971-540; E-mail: gcamoin@cerege.fr

0037-0738/99/$ – see front matter
PII: S0037-0738(99)00045-7

1. Introduction

Microbialites are "organosedimentary deposits that have accreted as a result of a benthic microbial community trapping and binding detrital sediment and/or forming the locus of mineral precipitation" (Burne and Moore, 1987). Based on internal structure, microbialites have been subdivided into stromatolites (fine, more or less planar lamination), thrombolites (clotted texture), cryptic microbialites (vague, mottled or patchy texture), oncolites (concentric laminations) and spherulitic microbialites (spherular aggregates). In modern and Quaternary marine environments, microbialites include both stromatolitic buildups or mats and lithified micrite crusts (laminated or thrombolitic).

Since the 80s, modern marine stromatolite buildups have been reported in high-energy settings of Bahamas, both on the platform margin of Schooner Cays (Dravis, 1983), in channels in the vicinity of Lee Stocking Island (Dill et al., 1986), and in subtidal tidal passes, subtidal sandy embayments, and intertidal beaches (Reid and Browne, 1991; Reid et al., 1995; Macintyre et al., 1996).

Lithified micritic crusts, generally regarded as microbialites, have been described in Quaternary reef tracts, mainly from the walls of the deeper forereef (Moore et al., 1976; James and Ginsburg, 1979; Land and Moore, 1980; Brachert and Dullo, 1991; Dullo et al., 1998), in lagoonal to intertidal settings (Jones and Hunter, 1991), and in shallow-water caves (Macintyre, 1984; Zankl, 1993; Reitner, 1993; Reitner et al., 1995). The occurrence of lithified micritic crusts in Quaternary reef frameworks has been previously reported by Marshall (1983, 1986) and Macintyre and Marshall (1988), but these authors did not assign a microbial origin to these crusts and noted that the evidence of 'algal mats' is only circumstantial. Microbialites associated with high-energy coralgal frameworks were reported by two of us (Montaggioni and Camoin, 1993; Camoin and Montaggioni, 1994) in drill cores penetrating the barrier reef complex off Tahiti and adjacent lagoonal patch-reefs. Since then, similar microbialites have been described in other Holocene shallow cryptic framework environments from the Caribbean (Zankl, 1993; D.J.W. Bosence pers. commun., 1994), the Great Barrier Reef (Webb, 1996; Webb and Jell, 1997; Webb et al., 1998), the Indian Ocean (Camoin et al., 1997), and Vanuatu (SW Pacific; Cabioch et al., 1998).

However, most of the lithified micritic crusts reported in Quaternary reef tracts are small structures that presumably played a limited role in reef accretion. In the Tahiti cores, the widespread development of framework microbialites is therefore paradoxical, because they form a major structural and volumetric component of the postglacial reef sequence. This paper deals with the nature, sedimentological role, and environmental significance of the microbialites, through analysis of facies distribution in time and space, examination of microbialite structure, and geochemical (stable isotopes, major and trace elements) and biochemical analyses (amino-acid composition) carried out on the 50–120-m-thick cored postglacial reef sequence.

2. Setting

Tahiti is a volcanic island (2241 m maximum altitude) situated at 17°50′S and 149°20′W in the Society Archipelago (French Polynesia, central Pacific Ocean). The volcanic activity has been dated at 1.367 ± 0.016 Ma to 0.187 ± 0.003 Ma (Le Roy, 1994). The environmental setting is described in Delesalle et al. (1985) and summarized in Camoin and Montaggioni (1994).

Tahiti is surrounded by discontinuous fringing reefs that grade locally into a chain of barrier reefs, locally enclosing a narrow back-reef area. The barrier reef complex has been subdivided into three reef zones, from the open sea landwards (Camoin and Montaggioni, 1994; Cabioch et al., 1999):

(1) The outer reef slope consists of coral-built spurs and grooves with abundant branching and massive scleractinian corals (robust acroporids, montiporids, pocilloporids and poritids) and hydrocorals (milleporids); associated framebuilders are coralline algae and vermetid gastropods.

(2) The reef flat zone is relatively narrow (130 m in maximum width) and consists of three distinct subzones. The outermost subzone (reef crest) is dominated by encrusting coralline algae (mostly *Hydrolithon*) associated with robust-branching corals. The intermediate subzone (patchy reef flat) exhibits scattered coral heads including branching acroporids

and pocilloporids, and massive poritids. In the innermost subzone (rubble reef flat), the floor is chiefly covered by coralgal rubble and living coral colonies are rare (*Acropora*, *Porites*). The reef flat is connected to the back-reef floor through a gently dipping biodetrital talus apron.

(3) The back-reef zone corresponds to a 1-km-wide bay with a maximum depth of 20 m. Two large flat-topped patch reefs of about 90,000 and 15,000 m^2 areal extent, respectively, occur in the central part of the back-reef zone. Their windward slopes are steep with nearly vertical drop-offs along the northern and western margins and relatively gentle leeward slopes. In terms of zonation, the tops of these patch-reefs correspond to an exposed reef flat zone dominated by robust-branching acroporids.

3. Methods

The barrier reef complex facing Papeete was drilled in 1990 (P6 drill hole), 1992 (P7) and 1995 (P8, P9 and P10) (Fig. 1) by the ORSTOM team at Tahiti using various coring systems, but principally a Sedidrill 500. Cores with diameters ranging from 47.6 to 63.5 mm were recovered from two vertical (P6 and P7) and three inclined (P8 at 33° from vertical; P9 and P10 at 30° from vertical) drill holes through the outer barrier reef flat. Drill holes reached depths ranging from 50 m.b.r.s. (metres below reef surface) (P6) to 120 m.b.r.s. (P7). The drill holes are aligned along a 2500-m-long transect on the barrier reef. Drill holes P9 and P10 are located at the edge of the Papeete Pass, which corresponds to the entrance of the harbour. Recovery was dependent upon framework type and on the size of internal cavities,

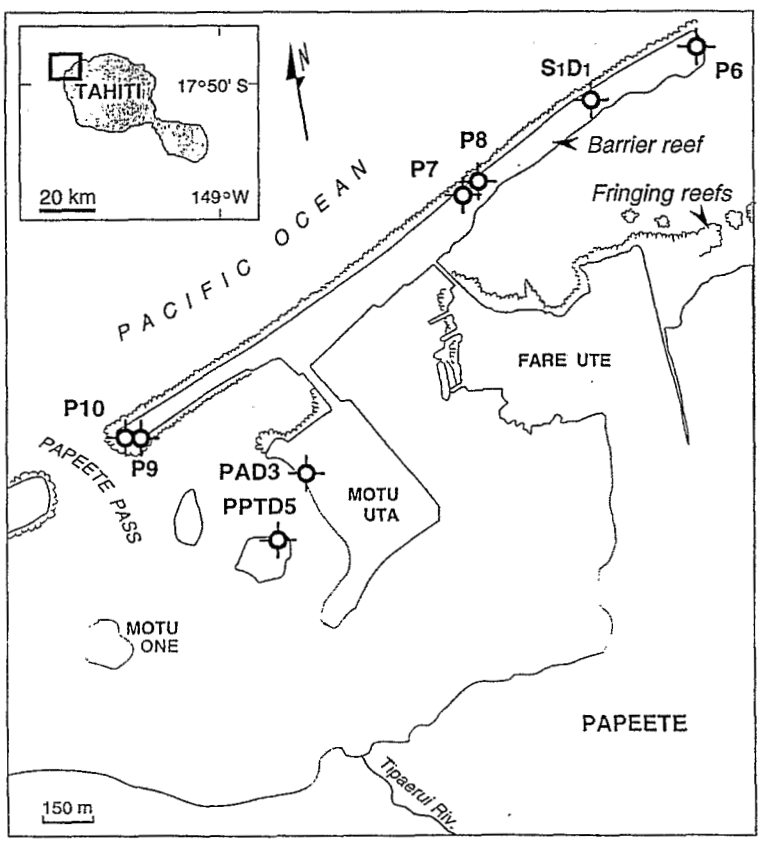

Fig. 1. Location map of drilling sites on the barrier reef (holes P6, P7, P8, P9, P10, S_1D_1) and lagoonal patch reefs (PAD3, PPTD5) in Tahiti.

but ranged from 50 to 95%; sections with poor or no recovery generally correspond to unconsolidated sands. During drilling operations, the tube barrel was advanced in 1.5 m steps; core depths were estimated with ±0.3 m accuracy.

Over 300 thin-sections were prepared from cores and 30 samples, some of them gently etched, were examined with a Hitachi S 570 scanning electron microscope. Microsamples were taken from microbialites and corals using a miniature lathe fitted with a 0.6-mm-diameter dental drill; the drilling routine was observed under a binocular microscope.

Stable isotope analyses (carbon and oxygen) on coral and microbialite samples were performed on a FINNIGAN MAT 252 connected to an online carbonate preparation line (Carbo-Kiel – single sample acid bath) and on a FINNIGAN MAT 251 mass-spectrometer coupled with a standard 'Bremen Carbonate Device'. Reproducibility is 0.04‰ PDB for $\delta^{18}O$ and 0.03‰ PDB for $\delta^{13}C$.

Trace element analyses were conducted by atomic absorption on an IL 551 apparatus. After crushing, samples were washed with distilled water to remove interstitial water. After this pretreatment, samples were dissolved in 1 N acetic acid. The accuracy of measurements of trace element concentrations ranges from 2 to 5%.

Polished thin-sections of microbialite crusts were analyzed by double wavelength dispersion spectrometry using a CAMEBAX microprobe analyzer for quantitative determination of major, minor and trace elements and element mapping.

Biochemical analyses were carried out on coral and microbialites sampled at several depths (8, 9, 11, 19 and 54 m deep). Samples were cut and cleaned with a miniature lathe fitted with a 0.6-mm-diameter dental drill. After crushing, millimetre-sized fragments were cleaned in ultrasonic bath and Na-hypochlorite to remove outer organic matter. They were rinsed with MilliQ water, dried at 30°C, powdered in a crusher, and then decalcified with acetic acid (pH 4, 15–20 H automatically controlled by a titrimeter) and centrifuged to remove insoluble compounds. The soluble organic matter was filtered and separated from Ca-salts by a desalting gel filtration chromatography with a PHARMACIA G25 (UV detection at 280 nm) and then vacuum-concentrated, ultrafiltered (MilliQ water; Filtron 3K cells), and freeze-dried. Then, organic matter was subject to 6 N HCl hydrolysis (24 h, 110°C in free-air sealed tubes), dried by evaporation (SpeedVac) and extracted with phenyl-isothiocyanate (PITC). Amino-acid composition was determined by reversed-phase chromatography using a HPLC-Beckman system (Hypersil column C_{18} 5 μm, 250 × 4.6 mm, UV detection 254 nm). Relative concentrations in %mol and absolute weights were determined with respect to a standard (amino-acid kit Beckman) and the total weights of all hydrolysed proteins were normalized for 1 g of carbonate.

4. Internal reef structure

The volcanic substrate underlying the drilled reef has a general SW–NE slope of 6° (Deneufbourg, 1971). Below the barrier reef, the depth of the basaltic or terrigenous substrate ranges between 85.5 (P9) and 114 m.b.r.s. (P7), as it deepens towards the northeast. A basaltic subaerial lava flow in P7 has been dated at 549 ± 11 ka by K–Ar (see Bard et al., 1996). In P9 and P10, the basalt is overlain by brownish clay which may correspond to the weathering profile of the basalt; pockets of volcanic sand and silt also occur in the lower part of the postglacial reef sequence, especially in P9 (i.e. at 50–87 m.b.r.s., corresponding to the time span 10,500–13,700 yrs B.P.). Tentative correlations between the drill holes on the barrier reef and those in the Papeete harbour (Deneufbourg, 1971; Camoin and Montaggioni, 1994) suggest that the terrigenous deposits form a 18–45-m-thick wedge below the modern lagoon, thinning both seawards and landwards (Fig. 2). From the available dates in the various cores (Montaggioni, 1988; Camoin and Montaggioni, 1994; Bard et al., 1996), it appears that the modern lagoonal zone was flooded around 10,000 yrs B.P. and that the accumulation of terrigenous sediments shifted landward.

The overlying carbonate sequence is subdivided into two reef units separated by an unconformity with evidence of subaerial exposure (Fig. 3; see also Cabioch et al., 1999).

(1) The lower unit, Pleistocene in age, consists of recrystallized and karstified limestone and was recorded only in the southeastern part of the drilled

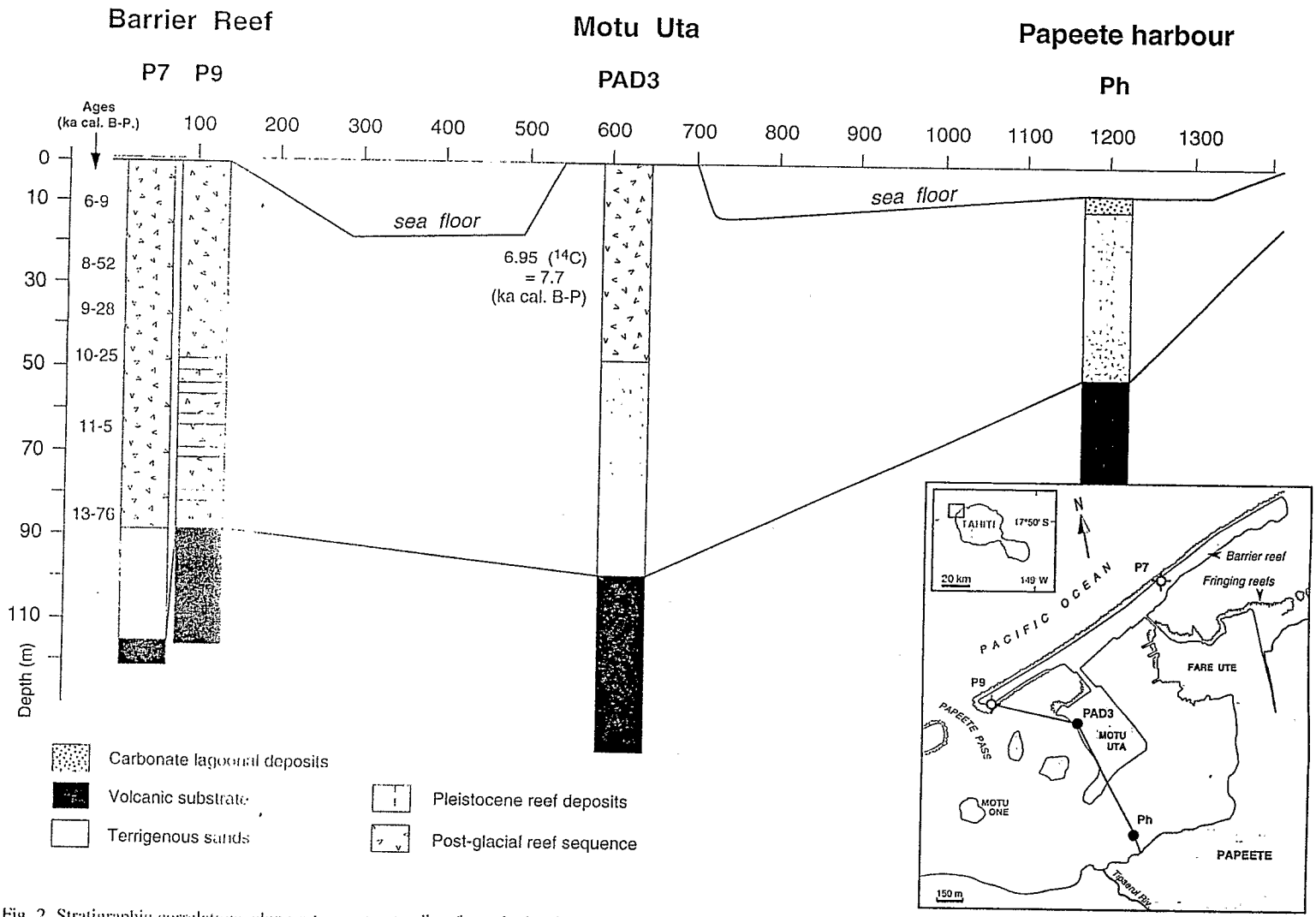

Fig. 2. Stratigraphic correlations along a transect extending from the barrier reef to Papeete. Data concerning lithology in drill holes performed in the lagoon (Motu Uta and Papeete harbour) are from Deneufbourg (1971).

zone (27 m thick in P7); it is absent in the area of P9 and P10 where the substrate is much shallower.

(2) The upper unit comprises in situ coralgal framework alternating locally with detrital beds (unconsolidated coral rubble and skeletal sands; terrigenous sands and silts), particularly in P9. Its thickness ranges from 85.5 to 92.15 m, respectively, in P9 and P8, and exhibits stratigraphically consistent ages ranging from 13,750 (±30) cal. yr B.P. at the base (P7: 83 m.b.r.s.; P8: 90 m.b.r.s.) to 2380 (±90) ^{14}C yr B.P. at the top of hole P6 (Bard et al., 1996). There is a clear differentiation of framework in this sequence in terms of gross facies distribution (Fig. 3) (see also Cabioch et al., 1999).

The lower part of this sequence, from its base to 65–70 m.b.r.s, contains two distinct coralgal assemblages. In the southwestern part of the barrier reef complex (P9 and P10), coralgal communities are predominantly composed of branching colonies of *Porites* cf. *nigrescens* and *P.* cf. *lichen* associated with scarce colonies of *Pocillopora*, *Porites* cf. *lobata* and faviids, indicating quiet to moderate energy conditions at variable depths, ranging from 6 to 30 m, depending on local ecological conditions (Kuhlman and Chevalier, 1986; Bouchon, 1996). In the central part of the barrier reef complex (P7 and P8), coralgal assemblages are composed of domal *Porites* (*Porites* cf. *lutea* and *P.* cf. *lobata*) mixed with scattered *Pocillopora* cf. *verrucosa* and tabular acroporids; branching red algae (*Lithophyllum*) form thin veneers (less than 1 cm) over *Porites* colonies. This community has been reported on modern outer reef slopes, in moderate- to high-energy conditions, at depths ranging from 6 to 15 m (Chevalier, 1978; Done, 1982; Faure, 1982), but also on the outer reef flats of atolls and on the windward zone of lagoonal pinnacles (Faure and Laboute, 1984; Kuhlman and Chevalier, 1986; Bouchon, 1996).

The prevailing coralgal framework between 65 and 70 m.b.r.s. and the reef surface comprises massive branching species of the *Acropora* gr. *danai/robusta* and fewer *Pocillopora eydouxi* and *P. verrucosa*, heavily encrusted by coralline algae (mainly *Hydrolithon onkodes* and, to a lesser extent, *Neogoniolithon fosliei* and *Mesophyllum* sp.). Associated with the algae are sessile vermetid gastropods (*Serpulorbis annulatus* and *Dendropoma maximus*) and encrusting foraminifers (*Homotrema rubrum*, *Carpenteria* cf. *monticularis* and *Acervulina inhaerens*). Cavities, up to 10 cm in size, are common and are locally occupied by large fragments of the echinoid *Heterocentrotus trigonarius*. In modern environments, this association of corals, red algae and vermetid gastropods is characteristic of reef crests and upper reef slopes, that are exposed to strong wave action in water depths less than 6 m (for corals see: Faure, 1982; Veron, 1986; for algae: Adey, 1986). The cavity-dwelling echinoid *Heterocentrotus trigonarius* occurs in high-energy areas at depths of about 3 m (de Ridder, 1986).

A tabular branching *Acropora* community, recorded from 37.0 to 50.0 m and 35.1 to 36.5 m.b.r.s. in P6 and P7, respectively, consists mainly of *Acropora hyacinthus*, *A. cytherea* and *A. clathrata* with subordinate, plate-shaped *A. danai/robusta* ecomorphs and domal *Montastrea annuligera*. Coralline algae developed only as millimetre-thick crusts and include *Neogoniolithon* cf. *absimile*, *N. propinquum*, *Dermatolithon* cf. *tesselatum* and *Mesophyllum* cf. *prolifer*. In most modern Indo-Pacific reefs, such tabular *Acropora*-rich assemblages develop along outer slopes, at depths varying from 5 m to deeper than 15 m, according to local water energy levels (Faure, 1982; Bouchon, 1996).

Lithified micrite crusts described here form coatings over coral branches or fragments and also over related encrusting organisms (red algae and crustose foraminifers) throughout the cored reef sections (Fig. 3).

5. Microbialites

5.1. Distribution in cores

In all cored sections microbialites appear as a major structural and volumetric component and locally may form up to 80% of the rock. Microbialites clearly increase in overall abundance towards the southwest, in the vicinity of Papeete Pass at sites P9 and P10.

Microbialites are fairly abundant in the lower postglacial subunit (base to 65–70 m.b.r.s.) which is characterized by *Porites nigrescens* and *P. lichen* community (P9 and P10). Microbialites consist exclusively of millimetre- to centimetre-thick thrombo-

ıe area of P9
llower.
itu coralgal
al beds (un-
nds; terrige-
ts thickness
vely, in P9
sistent ages
at the base
±90) ^{14}C yr
6). There is
is sequence
3) (see also

m its base
oralgal as-
the barrier
mmunities
g colonies
en associ-
Porites cf.
derate en-
ng from 6
conditions
1996). In
x (P7 and
of domal
ra) mixed
ıd tabular
ium) form
colonies.
ern outer
nditions,
er, 1978;
outer reef
lagoonal
man and

ween 65
mprises
ora gr.
axi and
ıe algae
r extent.
). Asso-
stropods
aximus)
rubrum,

Carpenteria cf. *monticularis* and *Acervulina inhaerens*). Cavities, up to 10 cm in size, are common and are locally occupied by large fragments of the echinoid *Heterocentrotus trigonarius*. In modern environments, this association of corals, red algae and vermetid gastropods is characteristic of reef crests and upper reef slopes, that are exposed to strong wave action in water depths less than 6 m (for corals see: Faure, 1982; Veron, 1986; for algae: Adey, 1986). The cavity-dwelling echinoid *Heterocentrotus trigonarius* occurs in high-energy areas at depths of about 3 m (de Ridder, 1986).

A tabular branching *Acropora* community, recorded from 37.0 to 50.0 m and 35.1 to 36.5 m.b.r.s. in P6 and P7, respectively, consists mainly of *Acropora hyacinthus*, *A. cytherea* and *A. clathrata* with subordinate, plate-shaped *A. danai/robusta* ecomorphs and domal *Montastrea annuligera*. Coralline algae developed only as millimetre-thick crusts and include *Neogoniolithon* cf. *absimile*, *N. propinquum*, *Dermatolithon* cf. *tesselatum* and *Mesophyllum* cf. *prolifer*. In most modern Indo-Pacific reefs, such tabular *Acropora*-rich assemblages develop along outer slopes, at depths varying from 5 m to deeper than 15 m, according to local water energy levels (Faure, 1982; Bouchon, 1996).

Lithified micrite crusts described here form coatings over coral branches or fragments and also over related encrusting organisms (red algae and crustose foraminifers) throughout the cored reef sections (Fig. 3).

5. Microbialites

5.1. Distribution in cores

In all cored sections microbialites appear as a major structural and volumetric component and locally may form up to 80% of the rock. Microbialites clearly increase in overall abundance towards the southwest, in the vicinity of Papeete Pass at sites P9 and P10.

Microbialites are fairly abundant in the lower postglacial subunit (base to 65–70 m.b.r.s.) which is characterized by *Porites nigrescens* and *P. lichen* community (P9 and P10). Microbialites consist exclusively of millimetre- to centimetre-thick thrombo-

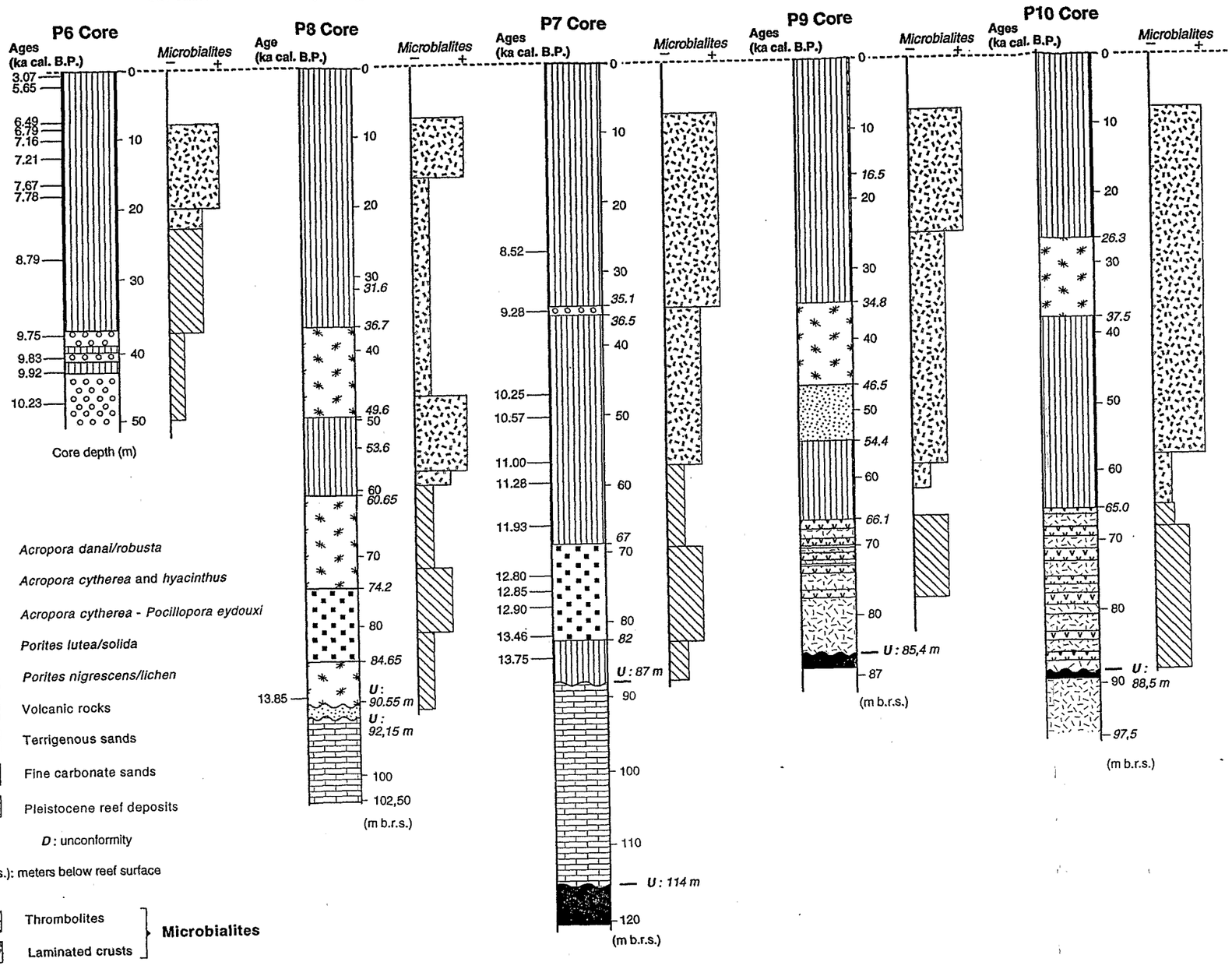

Fig. 3. Lithology, radiometric dates and distribution of coral assemblages and prevailing microbialite types in cores P6, P7, P8, P9 and P10.

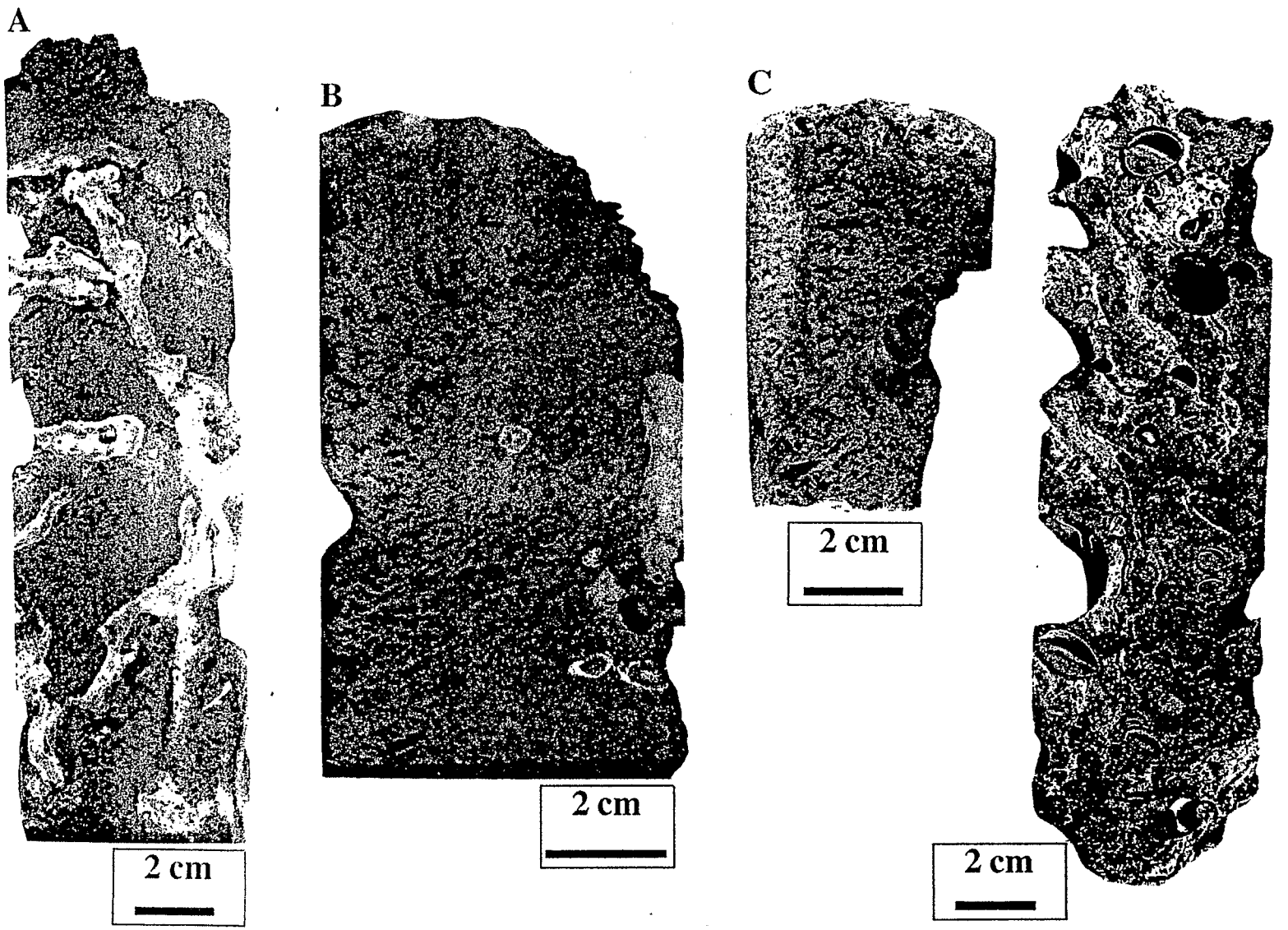

Fig. 4. Features of polished slabs. (A and B) Compound microbialite crusts occurring in tabular branching *Acropora clathrata* association where thrombolites form the last stage of encrustation. Core P6: 34.3 m (A) and 34.5 m (B). (C) Detail of a thrombolite crust developing centripetally at the edge of a faviid coral colony (*Favia stelligera*). Core P8; 28.7 m. (D) Polished slab showing bivalve borings in microbialites and red algal crusts. Core P9; 22.1 m.

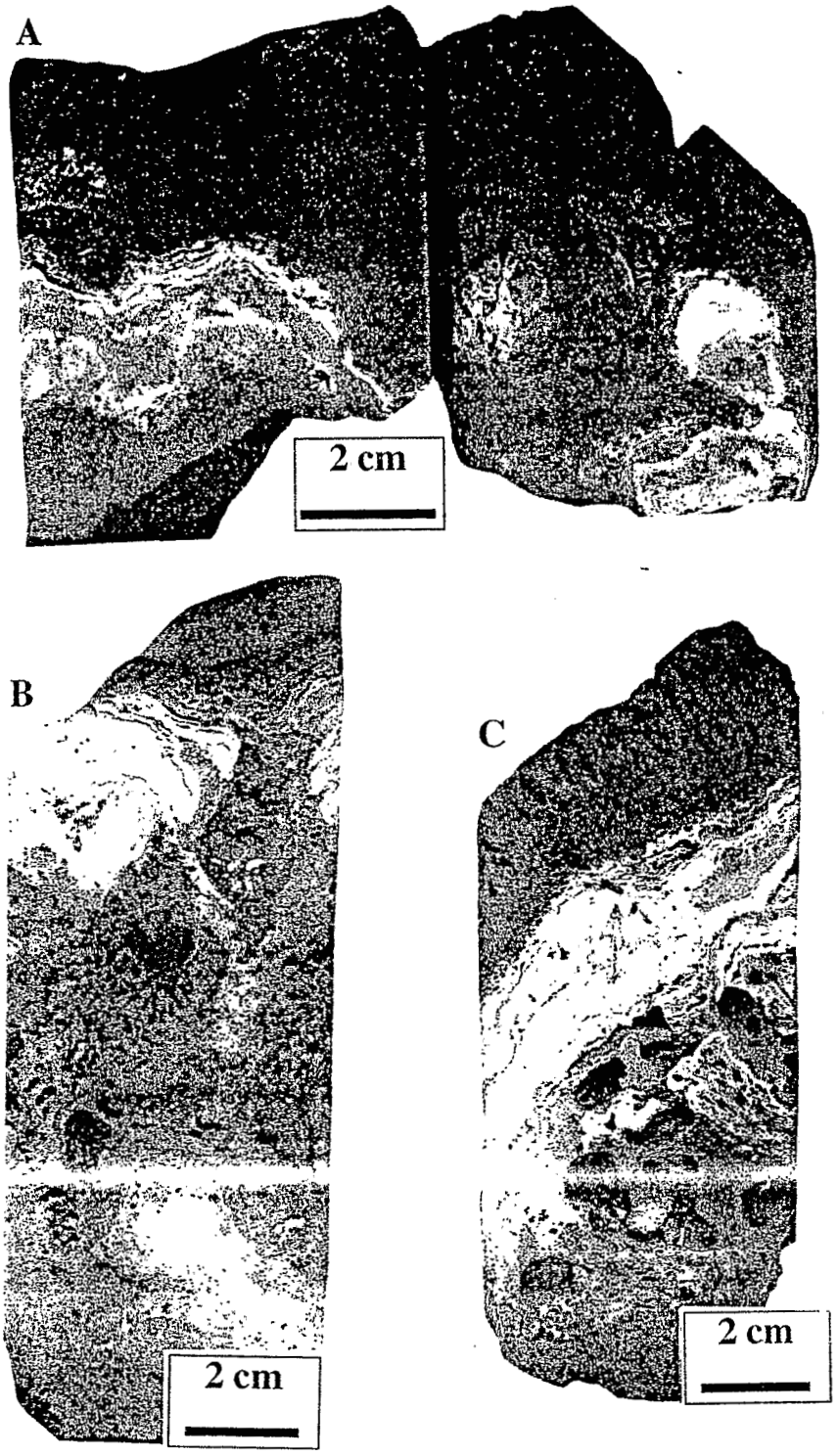
A
2 cm
B
2 cm
C
2 cm

lite crusts, generally growing over millimetre-thick red algal crusts or, more rarely, directly over coral branches (Fig. 3).

Microbialites are widespread in the upper subunit (65–70 m.b.r.s. to the modern reef surface) at all sites which is characterized by the development of the reef crest *Acropora* gr. *danai/robusta* association, but microbialite abundance decreases sharply in the uppermost 7 m, where they are restricted to thin thrombolite crusts in small pores (Fig. 3). Maximum microbialite abundance occurs between 16 and 7 m.b.r.s. in P7 and P8, between 26 and 7 m.b.r.s. in P9, and between 56 and 7 m.b.r.s. in P10 (Fig. 3). Microbialites in this upper subunit, generally consist of compound crusts up to 20 cm thick, in which laminated layers prevail. Thrombolites generally form the last stage of encrustation in large pore spaces but also occur in smaller cavities, such as borings in corals and red algal crusts.

5.2. Morphology and structure

The microbialites represent the last stage of encrustation and significantly reduced porosity within the large interskeletal cavities (average volume of 40%), thus restricting the space available for subsequent internal sedimentation and cementation. In addition, they formed in closed to semi-closed microcavities including sponge and bivalve borings in corals and red algal encrustations. Two types of crusts occur in Tahitian reef cores (i.e. laminated crusts and clotted micritic masses = thrombolites; Figs. 4–6).

XRD analysis indicates that the microbialites are composed of microcrystalline high-Mg calcites containing 7–16 mol% $MgCO_3$; traces of aragonite derive from the incorporation of comminuted skeletal fragments.

Laminated crusts are millimetre to centimetre thick, locally up to 20 cm thick in large interskeletal cavities. The crusts are characterized by planar or wavy laminae (Fig. 5A) that may have little lateral persistence; surfaces generally display bulbous or domal accretions. Their distribution suggests that crusts grew upwards or outwards from pore margins (Fig. 6B). Their internal structure consists of clotted to dense micrite that may include some traces of straight to gently curved micritic tubes 5–15 μm in diameter (Camoin and Montaggioni, 1994). These laminated crusts include horizontally oriented brownish to black films, 10–30 μm thick overlying microcorroded surfaces. Under UV-light these films do not display any fluorescence, but the underlying micritic laminae are characterized by an increasing fluorescence toward the film. Microprobe analyses and histochemical argentamin staining demonstrate that these crusts lack carbonates, but are rich in Mn, Fe, Mg, Si, Al and S.

The thrombolites consist of closely spaced and vertically and laterally intergradational micritic masses that range from narrow millimetre-sized upward-radiating shrubs to broader dendritic clusters up to 1 cm high (Fig. 4B,C and 5B). Multiple generations may be closely packed and merge into micritic crusts up to 3 cm thick. These micritic accretions form almost isopachous crusts with sharply defined outer margins (e.g. Fig. 4B and 6A). Thrombolites display a mottled to clotted internal fabric wherein dense micritic films are commonly interlaminated. The micritic masses are generally surrounded by isolated or interconnected irregular cavities, partly filled with fine-grained skeletal sands and terrigenous silt (Fig. 7A,C). Clots and peloids, 5–50 μm in diameter, may form networks where irregular microscopic pores which are interpreted to be primary voids in the coatings may give a 'spongy' appearance to the micritic masses (Fig. 7D). These pores are generally lined by thin isopachous fringes of bladed high-Mg calcite.

Both types of coatings commonly occur together in compound crusts where thrombolites generally form the last stage of encrustation (e.g. Fig. 4A and Fig. 6). Phosphatized grains and thin phosphate laminae commonly occur in both types of coatings.

Fig. 5. Features of polished slabs. (A) Dense microbial crusts displaying planar or wavy laminae and characterizing the reef-edge *Acropora* gr. *danai/robusta* coral association. Core P6: 12.9 m. (B) Compound microbialite crusts where thrombolites form the last stage of encrustation. Core P6: 14.2 m. (C) Dense microbial crust coating a thick red algal crust and characterized by the development of columnar accretions at the top. Core P6: 15.2 m.

Fig. 6. (A and B) Core surfaces showing thick compound microbialite crusts filling primary cavities of a *Pocillopora eydouxi* framework. Microbialites include dense laminated crusts that developed centripetally from the margins of the pores and thrombolites which form the last stage of encrustation. Core P10; 11.48 m.

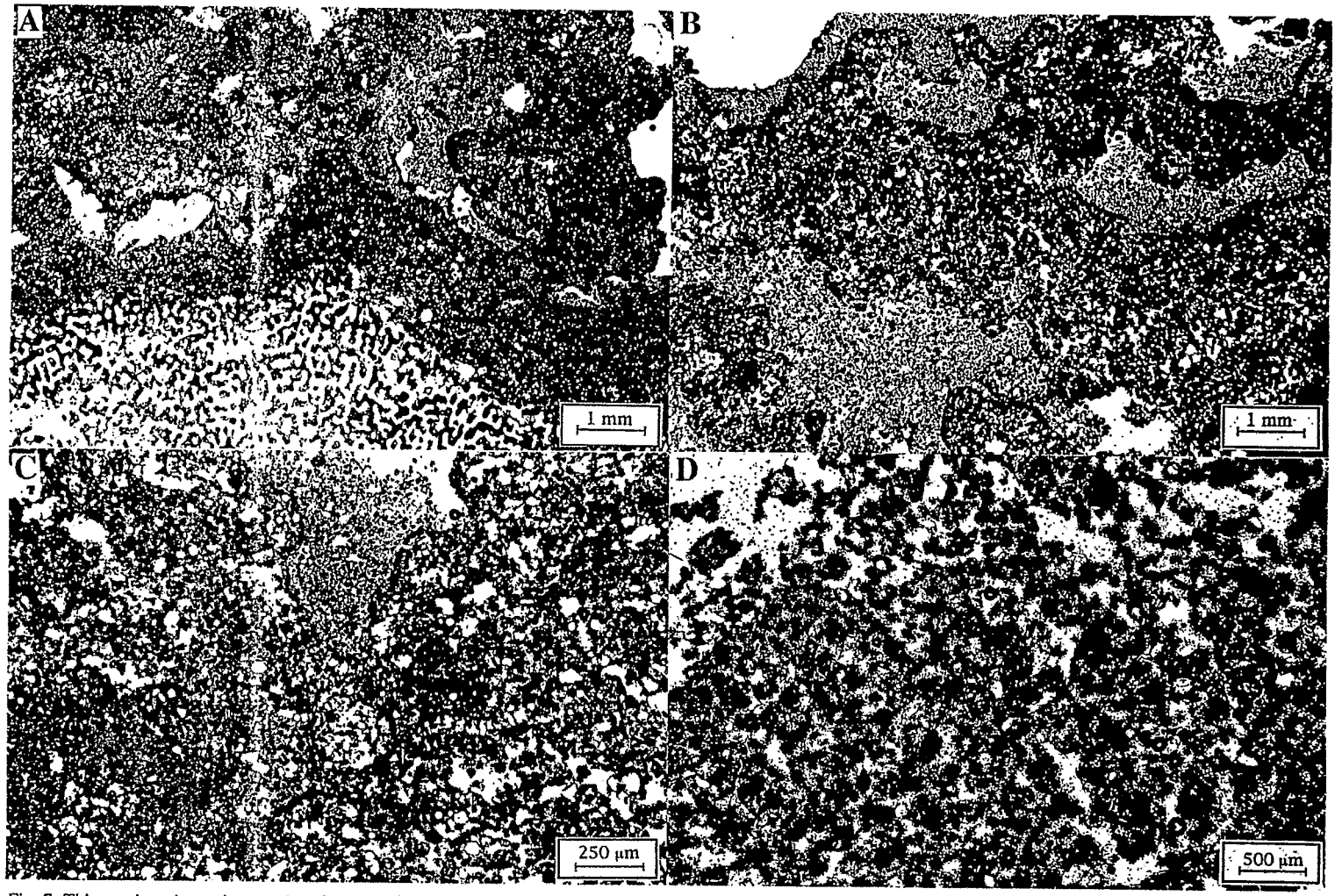

Fig. 7. Thin-section photomicrographs of microbialites. (A–C) Close-up of a thrombolite coating a coral skeleton and displaying club-shaped and domal microbial micritic accretions (dark). Irregular primary cavities between microbial accretions are partially filled with internal sediment. Core S_1D_1; 10.1 m. (D) Close-up of a thrombolite crust displaying a typical peloidal to clotted microfabric. Irregular microscopic pores within the fabric are typically lined by a thin, isopachous fringe of bladed high-Mg calcite crystals. Core S_1D_1; 10.1 m.

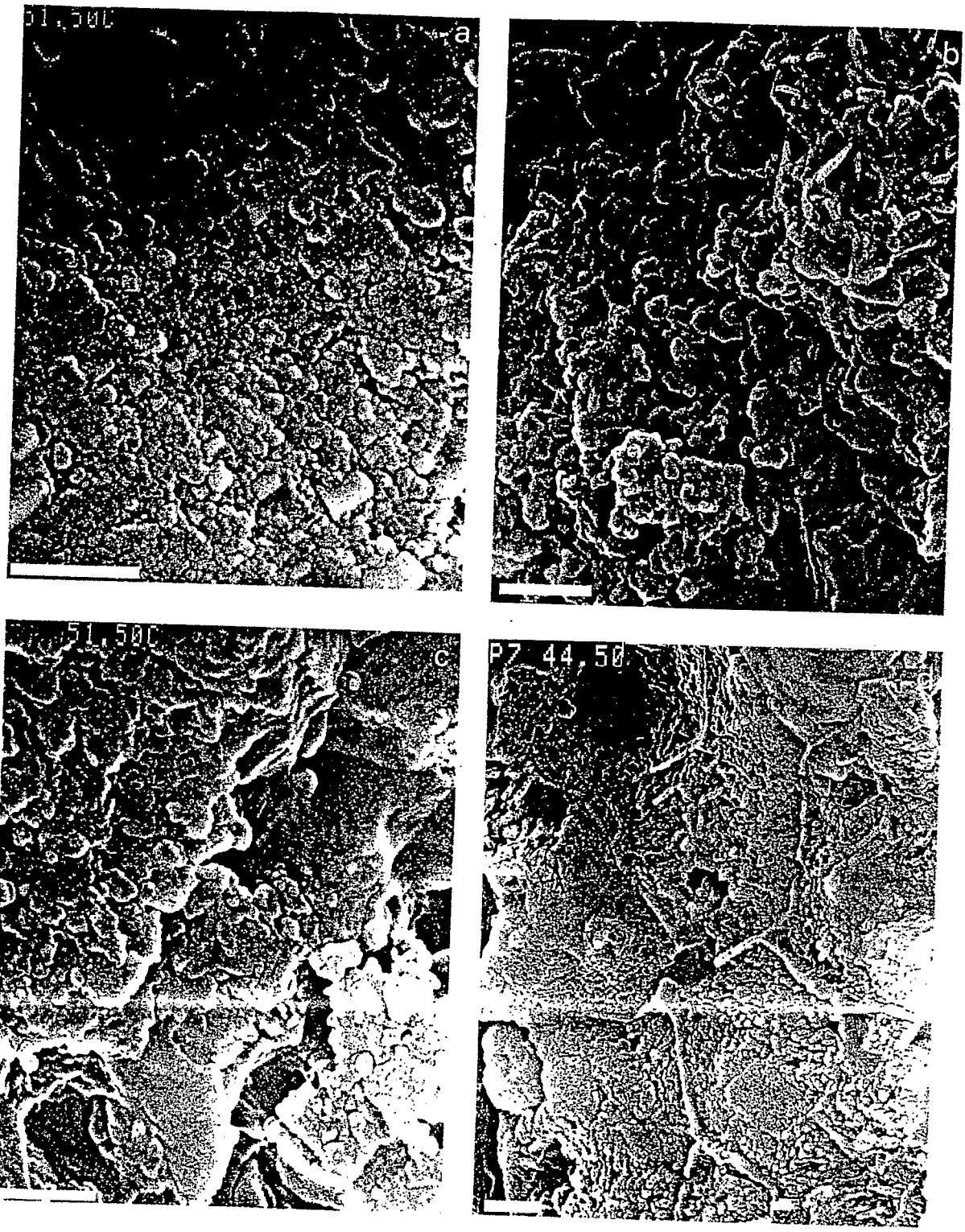
a
b
c
d

but are generally more abundant in the lower part of the crusts. Microcavities, up to 1 cm in size, are commonly present along the contact between the two types of layers and seemingly represent primary voids. The occurrence of encrusting organisms (bivalves, worms) locally between thrombolite and laminated layers in some compound micritic crusts suggests a local pause in the microbialite growth. Juvenile gastropods and bivalves (including *Trocha* and pectinids) occur in the microbialites and also in pores. Crusts are bored by sponges, lithophagid bivalves and microborers (Fig. 4D), and their outer surfaces are typically encrusted by serpulid worms and small bivalves.

5.3. Ultrastructure

Microbialites are typically composed of 0.1–0.2-μm-sized rounded crystallites which are typically closely packed in aggregates, grape-like clusters and swarms encrusted in very small calcite grains (20–50 nm) to form very fine micrite (0.5–2 μm) with anhedral crystal shapes (Figs. 8 and 9). Three-dimensional objects protrude from calcite microcrystals: (1) straight to gently curved filaments and micritic tubes with variable diameters (5–15 μm); and (2) micrometre-sized (0.5–2 μm) straight to gently curved filaments or straight rods to tiny ovoid bodies. Although the latter objects typically occur as isolated remnants, some aggregates and clumps reaching few micrometres in diameter are apparent.

Gradual downward changes in the ultrastructure of microbialites are recorded within the core sequence. These 'ageing' processes consist of the precipitation of successive calcite layers around former anhedral microcrystals, entombing the 0.1–0.2-μm-sized carbonate bodies (Fig. 10). The outer surfaces of the newly formed microcrystals are typically knobby. Polygonal structures (Fig. 8d) could correspond to remnants of initial organic substrates.

5.4. Geochemistry

Microbialites exhibit a narrow range of carbon and oxygen isotope values ranging from +2.05 to +3.92‰ $\delta^{13}C$ PDB (mean: +3.37‰; $n = 41$) with a standard deviation of 0.03‰, and −0.86 to +0.86‰ $\delta^{18}O$ PDB (mean: 0‰; $n = 41$) with a standard deviation of 0.04‰ (Fig. 10). These values are typical for a non-enzymatic fractionation and are close to those expected for calcitic cements precipitated at equilibrium with normal seawater (e.g. Mg-calcite cements from Mururoa atoll: +2 to +3.87‰ $\delta^{13}C$ and +0.70 to +1.16‰ $\delta^{18}O$; Aissaoui, 1988). There is no difference between isotopic composition of thrombolites and laminated crusts. A general positive covariation between carbon and oxygen isotope values in microbialites throughout the reef sequence is apparent. Our isotope data fall within the range of results obtained on similar crusts reported in Holocene reefs from Mauritius and Mayotte (mean: +2.73‰ $\delta^{13}C$ and −0.42‰ $\delta^{18}O$; Camoin et al., 1997), Jamaica (mean: $+3.0 \pm 1.0$‰ $\delta^{13}C$ and -0.5 ± 1.0‰ $\delta^{18}O$; Land and Goreau, 1970) and Heron Island (see Webb and Jell, 1997) (+3.48 ± 0.03‰ $\delta^{13}C$ and −0.02 ± 0.03‰ $\delta^{18}O$, this study). It is interesting to note that while $\delta^{13}C$ are similar, the $\delta^{18}O$ values of these reef framework microbialites are intermediate between those obtained from microbialites developed on reef foreslopes (e.g. ledge rocks; see Brachert and Dullo, 1991; Dullo et al., 1998) ($\delta^{18}O$: +0.90 to +2.32‰, this study) and in shallow-water caves (e.g. Lizard Island, GBR; $\delta^{18}O$: −1 to −0.5‰; Reitner, 1993; Reitner et al., 1995; Fig. 10).

Average carbon and oxygen isotope compositions of *Acropora* gr. *danai/robusta* coated by microbialites are lighter and vary widely from −3.58 to +1.96‰ for $\delta^{13}C$, and from −3.56 to −1.12‰ for $\delta^{18}O$. Their modern counterparts range from −2.37 to +0.41‰ $\delta^{13}C$ PDB and −4.79 to −3.15‰ for $\delta^{18}O$ (Camoin and Montaggioni, 1994).

Fig. 8. SEM micrographs of microbialites. (a–c) Views showing abundant 0.1–0.2-μm-sized spherical to subspherical bodies closely packed in aggregates, grape-like clusters and swarms encrusted in very small calcite grains (20–50 nm) to form very fine micrite (0.5–2 μm) with anhedral crystal shapes. (d) View showing the occurrence of polygonal networks which could correspond to remnants of the initial organic substrates. (a): sample P7 51.50; (b): sample 47.50; (c): sample P7 51.50; (d): sample P7 44.50. Scale bar: 1 μm on all photos. All samples are broken surfaces.

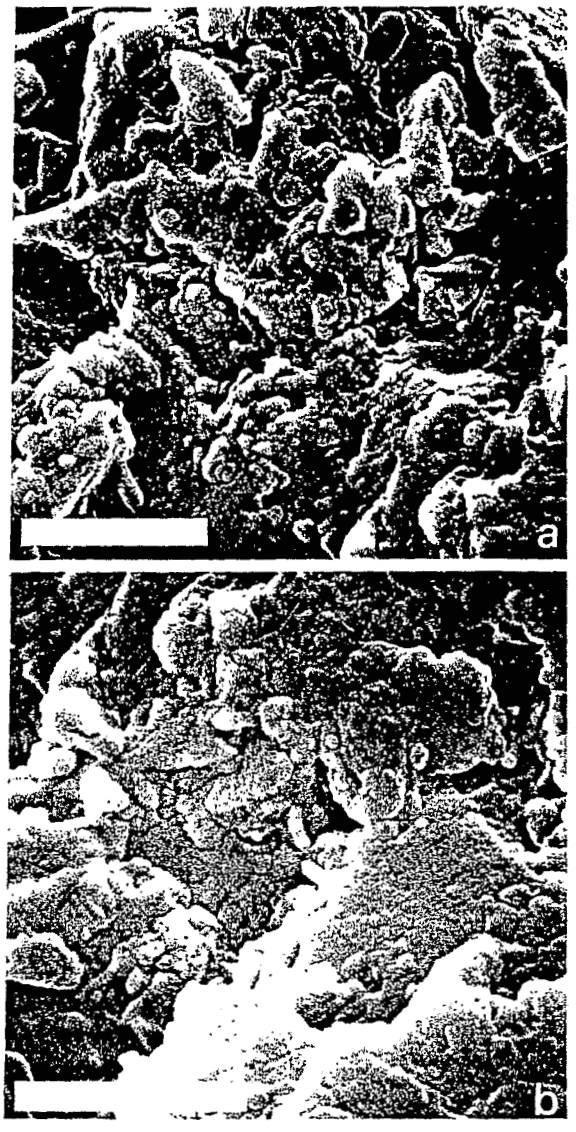

Fig. 9. SEM micrographs of microbialites. (a and b) Views showing the 'ageing' processes which consist of the precipitation of successive calcite layers around former anhedral microcrystals, entombing the [illegible] 0.2-μm-sized carbonate bodies. (a and b) sample P9 59.20. Scale bar: 1 μm on all photos.

The average chemical composition of the microbialites is reported in Table 1. The background values of Ca and Mg of microbialites range, respectively, from 44.7 to 47.7% and from 6.3 to 7.2% (Déjardin, 1996). The Mg/Ca ratio is almost constant, ranging from 0.11 to 0.14 and averaging 0.12. This value is consistent with those given for the precipitation of calcite from interstitial normal-marine waters (Folk and Land, 1975; Hardie, 1987). Sr concentrations vary considerably and apparently randomly from sample to sample, ranging from 1066 to more than 6000 ppm; Reitner (1993) reports values of 2000–2500 ppm Sr in microbialites from Lizard Island. The Sr/Ca ratio ranges generally from 0.0035 to 0.005. The concentrations of other cations (Mn, Ba, Al, Si, Fe) are generally lower than 500 ppm but record variations along the cored reef sequence in P6 and P7. Fe and Mn concentrations range from 174 to 473 ppm (average: 302 ppm) and from 38 to 155 ppm (average: 84 ppm), respectively, and exhibit an overall decreasing trend upwards (Fig. 11). The highest values for these two elements occur between 50 and 20 m.b.r.s., and a peak occurs at 10 m.b.r.s. (Fig. 11), coinciding with the highest concentrations in SiO_2 (above 1.3%) and Al_2O_3 (above 0.7%) (Déjardin, 1996). Below 50 m.b.r.s., concentrations of SiO_2 are lower, but still higher than those measured in samples shallower than 10 m.b.r.s. where a sharp decrease is recorded at 7 m.b.r.s. (Déjardin, 1996). Peaks in concentrations of Al, Si and Fe occur at 16, 12 and 7 m.b.r.s., respectively, in adjacent drill holes (Camoin and Montaggioni, 1994).

5.5. Biochemical analyses

5.5.1. Soluble matrices of acroporids

Amino-acid composition of soluble intraskeletal matrices of fossil versus modern robust-branching *Acropora* (Fig. 12) gives an estimate of the diagenetic alteration that could have affected the biochemical composition at depths where the microbialites were collected.

Significant changes in amino-acid composition concern mainly aspartic acid, glutamic acid and serine, which record a decrease in relative concentrations, whereas a slight increase in basic amino acids (lysine: histidine and arginine) occurs. These changes seem to occur very early, because they also are recorded in dead parts of modern coral colonies. Furthermore, there is no increase in glycine and alanine, which generally results from the degradation of other amino acids, nor is there excessive production of ammonium, which characterizes the deamination of all amino acids. These data suggest that the con-

Table 1
Average chemical composition (in ppm) and % $CaCO_3$ of microbialites

Depth (m)	Core	% $CaCO_3$	Trace elements					
			Ca	Mg	Sr	Mn	Fe	Mg/Ca
7	P6	92.41	310311	36617	1527	58	225	0.118
9	P6	94.24	311651	40515	1078	72	221	0.13
9	P6	92.84	310643	38520	1622	59	226	0.124
9	P6	84.8	338211	40585	2137	59	275	0.12
9	P6	95.29	309952	39054	1327	63	228	0.126
10	P6	81.35	330278	44918	1345	89	469	0.136
10	P6	92.9	303135	38801	1546	54	239	0.128
11	P6	92.42	303122	37587	2116	62	268	0.124
11	P6	94.05	314904	32120	2822	51	222	0.102
11	P6	92.97	316898	29788	3017	81	264	0.094
11	P6	96.84	299542	40738	1066	53	229	0.136
12	P6	95.54	296910	41567	1105	53	222	0.14
12	P6	95.86	319003	26158	4504	38	174	0.082
12	P6	94.19	297026	40395	1331	82	235	0.136
14	P6	96.46	302867	33315	2259	62	239	0.11
14	P6	93.22	304712	36565	1975	67	247	0.12
15	P6	93.58	310479	32290	2676	91	283	0.104
15	P6	94.46	301010	35519	1999	82	285	0.117
17	P6	94.11	303150	37591	1679	73	284	0.124
18	P6	91.97	307712	33233	2492	77	285	0.108
18	P6	92.85	304734	38396	1621	66	247	0.126
19	P6	92.91	305425	33597	2437	65	249	0.11
19	P6	93.3	305915	34263	1952	72	234	0.112
22	P6	93.97	301322	3495	2091	83	344	0.116
22	P6	94.32	295545	36056	2193	90	355	0.122
24	P6	94.34	302985	38782	1291	74	261	0.128
24	P6	94.2	306272	35528	1770	60	255	0.116
26	P6	94.02	305550	37277	1791	81	264	0.122
26	P6	93.64	303720	38269	1525	84	268	0.126
26	P6	95.02	295607	41976	1543	89	349	0.142
27	P6	93.58	313876	34526	2498	110	364	0.11
29	P6	91.73	289839	38259	1704	117	383	0.132
29	P6	90.77	297058	40400	1580	109	345	0.136
31	P6	91.78	307433	38737	1531	134	430	0.126
31	P6	91.03	307129	37470	1959	155	473	0.122
31	P6	93.81	289574	42278	1141	131	382	0.146
31	P6	92.04	316612	31661	2831	113	361	0.1
32	P6	92.52	307886	36331	2112	101	382	0.118
34	P6	93.59	298333	40573	1259	124	400	0.136
34	P6	93.49	312966	36930	1965	115	382	0.118
37	P6	94.13	312908	[illegible]	[illegible]	[illegible]	368	[illegible]
39	P6	94.37	325671	28659	4143	70	248	0.088
39	P6	93.41	311465	33638	2604	83	314	0.108
40	P6	94.17	313238	36962	1879	106	313	0.118
40	P6	92.25	319954	32635	2688	116	329	0.102
44	P6	93.54	317253	32360	2906	114	425	0.102
44	P6	94.99	317878	20344	5188	119	413	0.064
46	P6	96.22	306533	37397	1858	84	362	0.122
46	P6	95.55	302790	36940	1980	78	394	0.122
47	P6	92.72	302424	38710	1337	95	369	0.128
48	P6	95.48	310122	30392	2946	72	285	0.098
48	P6	96.92	333046	14654	6128	46	216	0.044
51	P7	92.2	297243	40533	1327	116	381	0.136
78	P7	96.62	317139	38057	1414	39	178	0.12

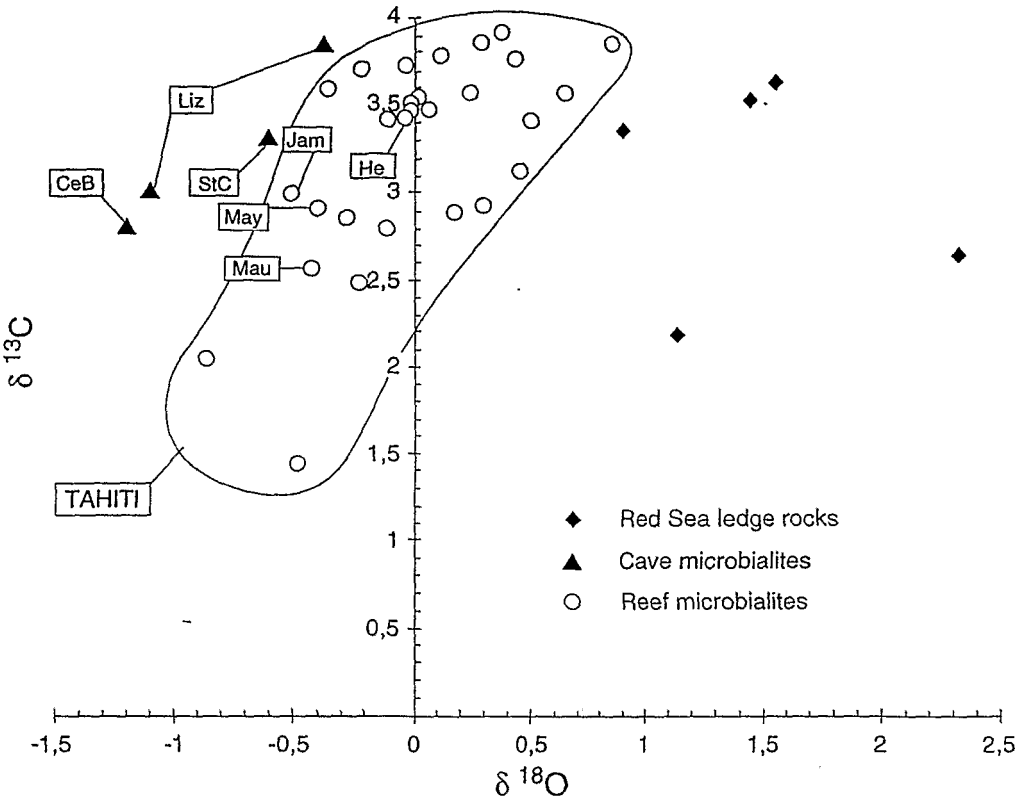

Fig. 10. Cross-plot of stable isotopic composition of microbialites, and Holocene and modern corals. Modern *Acropora* refer to samples taken from colonies on the present-day reef front at depths less than 5 m. Holocene *Acropora* and microbialites refer to samples taken at various levels from drilled Holocene sequences. *CeB* = Cebu; *Liz* = Lizard Island; *StC* = St. Croix; *Jam* = Jamaica; *Mau* = Mauritius; *May* = Mayotte; *He* = Heron Island.

ditions of preservation of the studied material are generally good. Changes in amino-acid composition of *Acropora* and microbialites (both thrombolites and laminated crusts) in the studied samples taken at various core depths are slight and are not considered significant (Fig. 13). In particular, there is no gradual decrease in aspartic acid or serine (i.e. the most unstable amino acids), or in absolute quantities of proteinaceous matrices, which could reflect an alteration gradient.

5.5.2. Compounds other than amino acids

The soluble matrices of all studied samples (including *Acropora*) include ornithine, which is common in decaying organic matter and is especially related to the degradation of arginine. All studied microbialites include the same non-identified compound (eluted with a retention time of 9.4 mn), which may be primary or the result of recombination or degradation. It could be characteristic of carbonates formed in microbial environments.

5.5.3. Composition of insoluble organic matrices

Insoluble matrices, including those in *Acropora* skeletons, have been greatly altered (leading to conditions close to the 'humic acids') in all studied facies. The prevalent components [illegible] and ammonia. Other compounds were identified with uncertainty and could represent muramic acid, which is present only in mureins of bacterial cell walls, and a possible product of the melanoidine type, which results from the recombination of amino acids and glucose. Diaminopimelic acid, which occurs exclusively in mureins of bacterial cells, methionine, and cysteine also occur in variable proportions. The only identified amino acids are alanine, leucine and

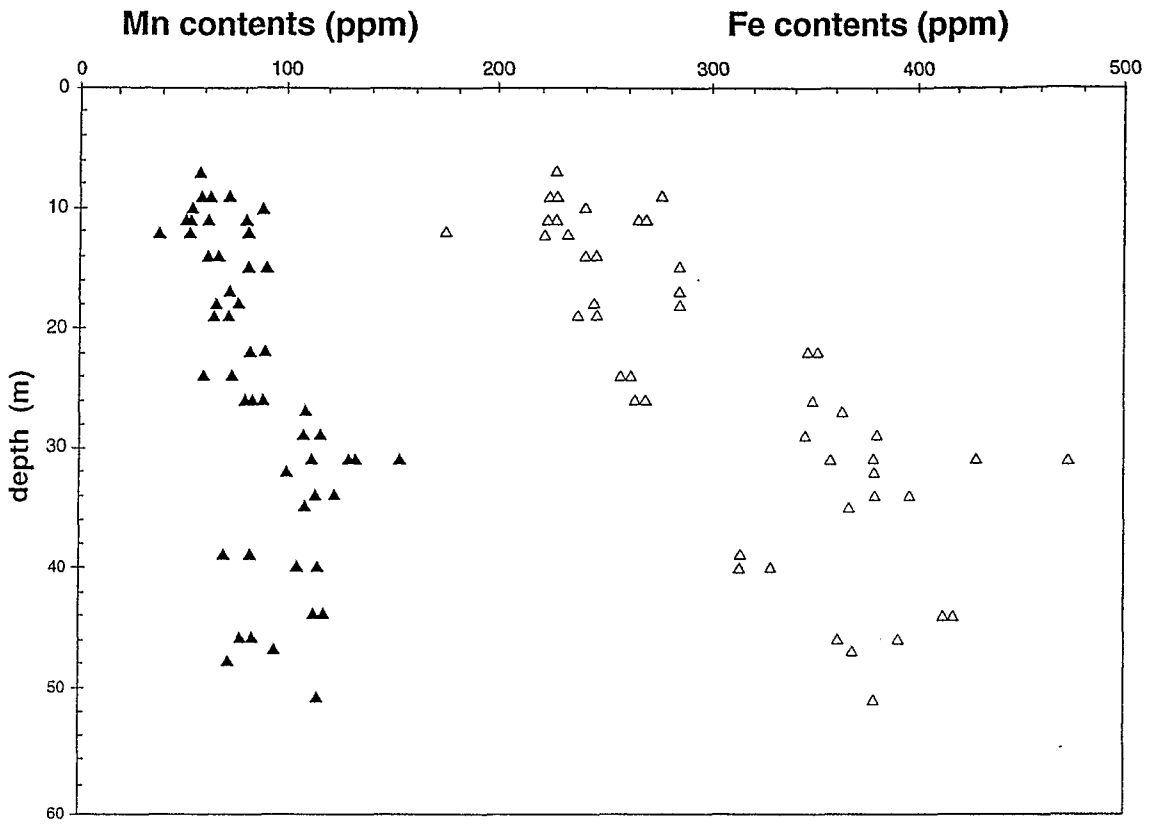

Fig. 11. Graphs of Mn and Fe content in microbialites (in ppm) vs depth in the Holocene reef sequence.

isoleucine, although traces of aspartic and glutamic acids occur locally.

5.5.4. Comparison between soluble matrices in Acropora and microbialites

Soluble matrices extracted from coral skeletons differ from those from microbialite crusts by: (a) higher concentrations of aspartic and glutamic acids (with the exception of sample P10/8.05 m) and of arginine; and (b) lower concentrations (less than [illegible] of hydroxyproline (see Table 1 and Fig. [illegible]). The weight of these proteinaceous compounds in their soluble matrices ranges between 1 and 3.5 μg/g of skeleton and are lower than those found in microbialite crusts.

5.5.5. Comparison between soluble matrices extracted from thrombolites and laminated crusts

Differences between relative compositions of the two microbialite types are slight. Glycine and alanine contents are higher in thrombolitic facies, whereas aspartic acid and hydroxyproline contents are higher in laminated crusts (Fig. 14). The two types of microbialites can be distinguished more easily when using absolute quantities of each amino acid expressed in ng/g of carbonate (Fig. 14) rather than relative concentrations in mol%. The proteinaceous compounds are seemingly more abundant in thrombolites than in laminated crusts.

6. Origin of microbialite crusts

We previously reported a suite of fabrics that characterize the microbialite crusts, including especially their typical growth forms and their great variations in thickness, lateral persistence and internal structure on small scale, which allow them to be interpreted as bio-accretionary features (Camoin and Montaggioni, 1994). The origin of microbialite

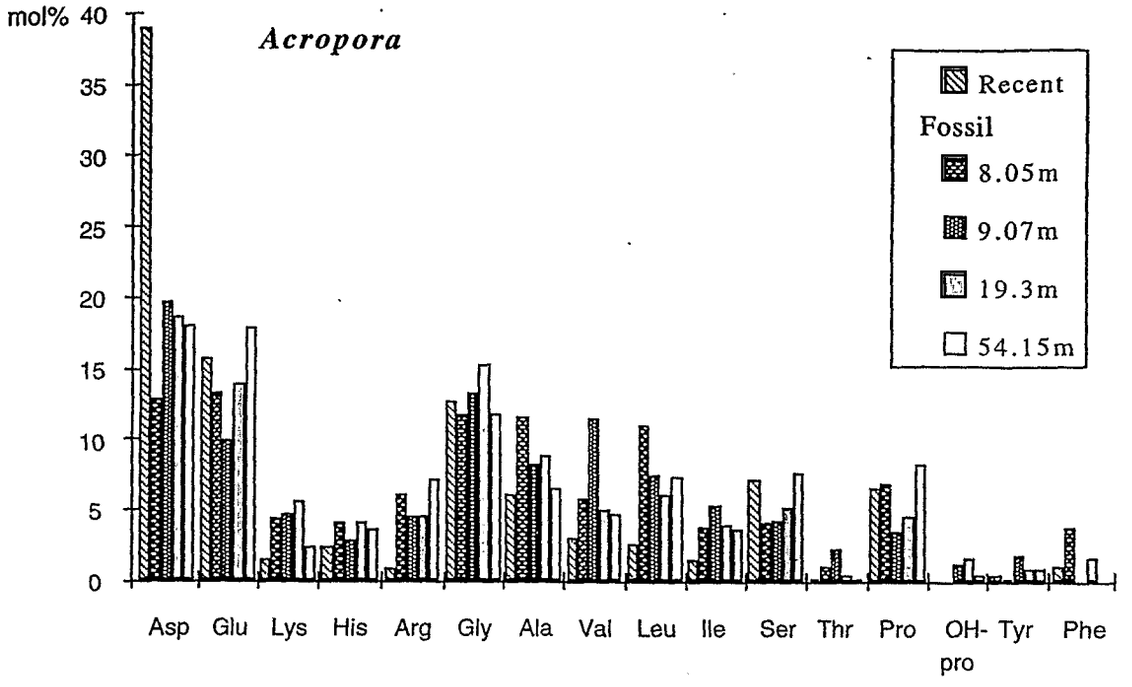

Fig. 12. Relative amino-acid composition of modern and Holocene *Acropora*. Major amino acids: *Asp* = aspartic acid; *Glu* = glutamic acid; *Ser* = serine; *Lys* = lysine; *His* = histidine; *Arg* = arginine; *Gly* = glycine; *Ala* = alanine.

crusts can be investigated through their ultrastructure and their biochemical composition, which are related to the composition of initial biological communities and mineralization processes involved in their development.

The origin of the largest filaments and tubes, characterized by large variations in size, is unknown, because such structures characterize many taxonomic groups. Similar microfossils have been described in laminar micritic crusts from the Red Sea foreslopes and, based on their size and mode of calcification, were interpreted as possible remnants of fungi or cyanobacteria (Reitner, 1993). Comparable micrometre-sized objects (0.5–2-μm-sized filaments, rods and oval bodies) are very likely bacterial remains.

The origin of the 0.1–0.2-μm-sized rounded crystallites is a critical problem in the interpretation of the crusts because they form the basic constructional element of the micrite, as it was also reported in similar microbialites (e.g. Lizard Island thrombolites; Reitner et al., 1995) and lithified micritic crusts occurring on reef foreslopes (e.g. Red Sea ledge rocks; Fig. 16). Similar crystallites have been referred to as calcified dwarf bacterial forms under a variety of terms among which 'nannobacteria' (Morita, 1988) is now the most popular (see Folk, 1993). Nannobacteria have been reported in many sedimentary deposits, where they seemingly play a prominent role in the precipitation of various carbonate minerals, including calcite, aragonite and dolomite (see Folk, 1993; Pedone and Folk, 1996; Vasconcelos and McKenzie, 1997). However, the nature of these very small carbonate bodies is still debated. Folk (1993) emphasized the bimodal size mixture of bacteria and nannobacteria in laboratory cultures and many recent and fossil sedimentary deposits as evidence for the biologic origin of the structures; he interpreted as-

Fig. 13. Relative amino-acid composition of microbialites and Holocene *Acropora*. Major amino acids: *Asp* = aspartic acid; *Glu* = glutamic acid; *Ser* = serine; *Lys* = lysine; *His* = histidine; *Arg* = arginine; *Gly* = glycine; *Ala* = alanine.

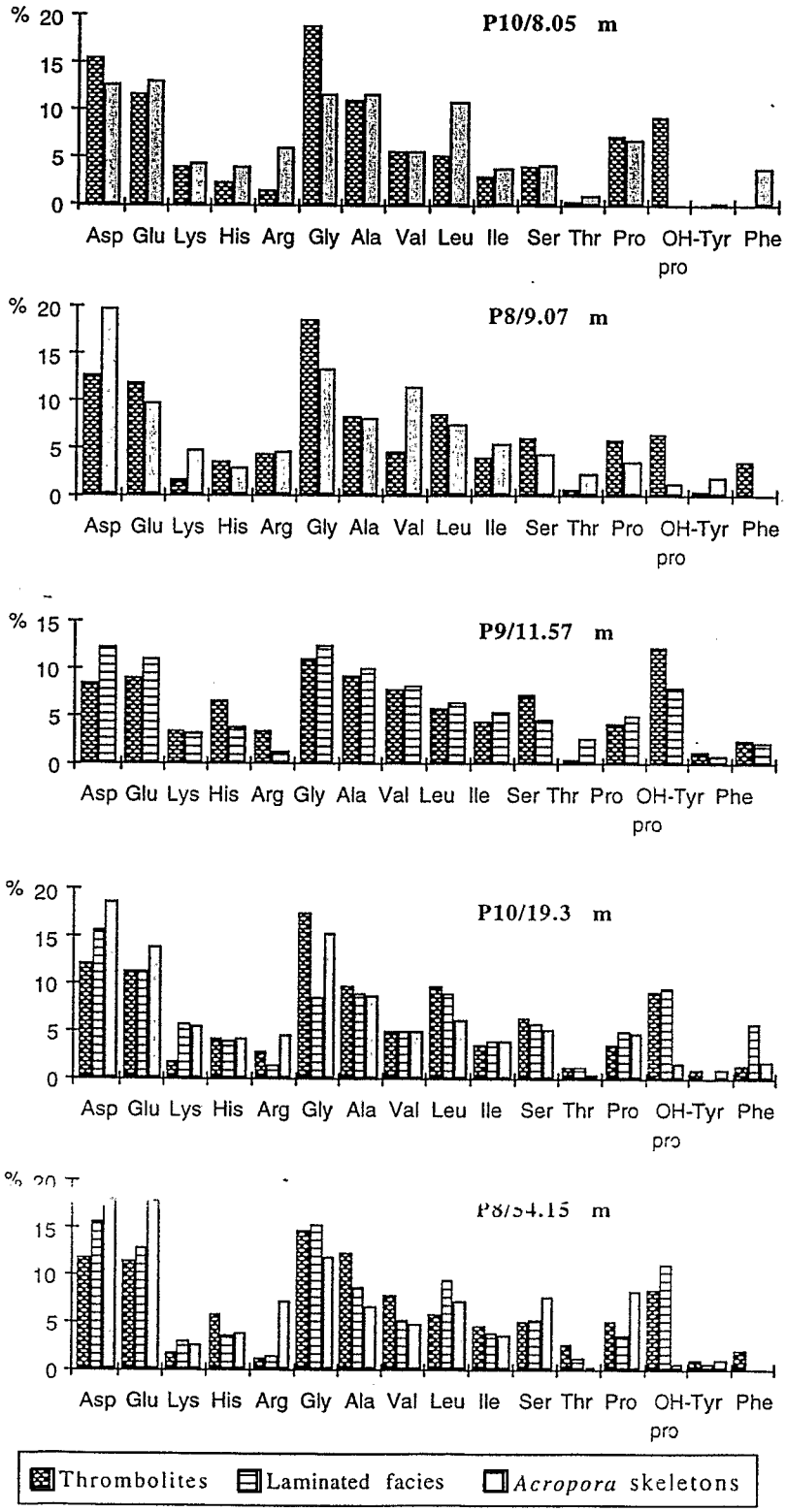
P10/8.05 m
P8/9.07 m
P9/11.57 m
P10/19.3 m
P8/54.15 m
%
Asp Glu Lys His Arg Gly Ala Val Leu Ile Ser Thr Pro OH-Tyr Phe pro
Thrombolites
Laminated facies
Acropora skeletons

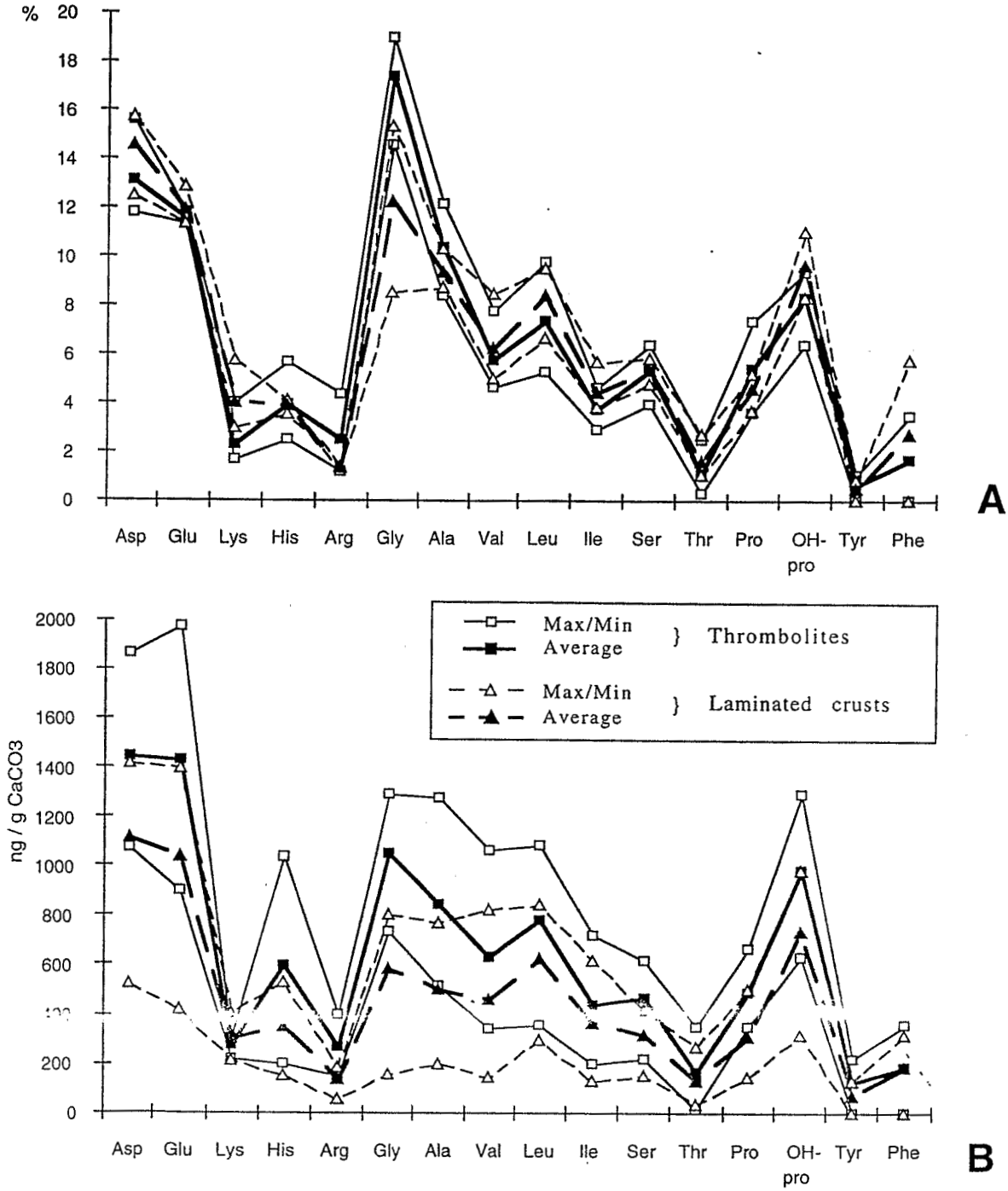

Fig. 14. Comparison between amino-acid composition of thrombolites and laminated crusts (maximum and minimum values): (A) concentrations in mol%; (B) amounts in ng/g. Major amino acids: *Asp* = aspartic acid; *Glu* = glutamic acid; *Ser* = serine; *Lys* = lysine; *His* = histidine; *Arg* = arginine; *Gly* = glycine; *Ala* = alanine.

sociated very small micrite crystals as calcified nannobacterial cells. Such a bimodal size distribution is present in the Tahiti structures and in other microbialite deposits (e.g. kopara; Défarge et al., 1996). In Quaternary travertines, Guo and Riding (1994) reported similar spherical bodies that they called 'bacteriform bodies' and interpreted them as remains of bacteria. They interpreted 'mini-micrites' as precipitates in associated biofilms through processes related to microbial life or death, based on similarities with bacterially precipitated micritic granules formed on, and close to, bacterial cells in laboratory experiments (Krumbein, 1979). The biological origin of nannobacteria also has been strengthened by culture experiments producing dolomite (Vasconcelos and McKenzie, 1997) and cultures from human, rabbit and bovine blood (see Gournay et al., 1999); furthermore, living nannobacteria are abundant in tropical reef environments (S. Ferrara-Guerrero, oral commun., 1998). Alternative interpretations for nannobacteria include bacterial parasites or spores (see Gournay et al., 1999). In contrast, still some authors did not assign a microbial origin to similar carbonate crystallites, interpreting them rather as by-products of the initial calcification of extracellular polymeric substances (EPS) (Reitner et al., 1995).

Within the gradational range of Tahiti microbialites, dendritic growth forms are probably the most striking features and closely resemble fabrics that have been interpreted as calcified cyanobacterial sheath material, or attributed to the activity of bacteria, lichens, algae or fungi (see review in Camoin and Montaggioni, 1994), the morphology being not indicative of systematic affinities. Furthermore, many microbialites, even in modern environments, retain little, if any, information concerning the organisms responsible for their formation. The prime evidence of microbial involvement may be obscured by rapid decay of microbial colonies or by the calcification of thick and diffuse, often degraded and homogenized, mucilaginous sheath material (see Riding, 1991). The Fe/Mn biofilms that occur in laminated crusts probably have a microbial origin. Similar Fe/Mn biofilms have been described in ledge rocks (Brachert and Dullo, 1991) and in cave microbialites (Reitner, 1993) where identified bacteria have affinities with *Siderocapsa* sp.

The relative scarcity of extraneous particles (e.g. terrigenous silt and sand, clay minerals, volcanic grains, peloids, ooids and skeletal debris) in the Tahiti crusts suggests that sediment trapping was much less important than calcification of organic mucilage associated with living or decaying organisms, and in-place, microbially mediated, precipitation of micrite. Furthermore, rapid lithification may be deduced from the presence in microbialites of borings (see also Camoin and Montaggioni, 1994). The trapping of grains on the crusts, even on vertical surfaces, suggests that the crust exterior was at one stage composed of a sticky mucilaginous material.

Défarge et al. (1996) demonstrated that microscopic three-dimensional organic networks inherited from sheaths of dead cyanobacteria and from other EPS of microbes in the deposits (filamentous or coccoid cyanobacteria, or bacteria) act as a matrix for calcification, initiating and supporting mineral growth (i.e. 'organominerals'); crystal nucleation is probably initiated at acidic sites (uronic, aspartic and glutamic acids), which are capable of binding divalent cations in the polysaccharide framework of mats.

Modern reef cave thrombolitic fabrics were interpreted as products of matrix-mediated calcification via reactive acidic organic Ca-binding macromolecules (including those forming a 'thin collagenous fibre network') with the addition of detrital material trapped in microbial and metazoan mucilage and associated biofilms (Reitner, 1993; Reitner et al., 1995; i.e. 'biologically matrix mediated' in the sense of Weiner et al., 1983). Zankl (1993) emphasized the role of bacteria and fungal hyphae in high-Mg calcite nucleation in similar crusts from St. Croix.

In modern microbial benthic deposits abundant quantities of mucilage are produced by bacteria, cyanobacteria, diatoms, eukaryotic algae and occasionally by associated invertebrates such as polychaetes, and also by fungi, corals and plant roots (see Défarge et al., 1996). In addition, Reitner et al. (1995) have stressed the importance of biofilms produced by sponges and noted the occurrence of fucose, which is characteristic of calcifying mucous substances.

The soluble organic matter extracted from Tahiti microbialites displays the characters reported in shallow-marine microbialites. The proteic compounds are abundant, with relative concentrations in aspar-

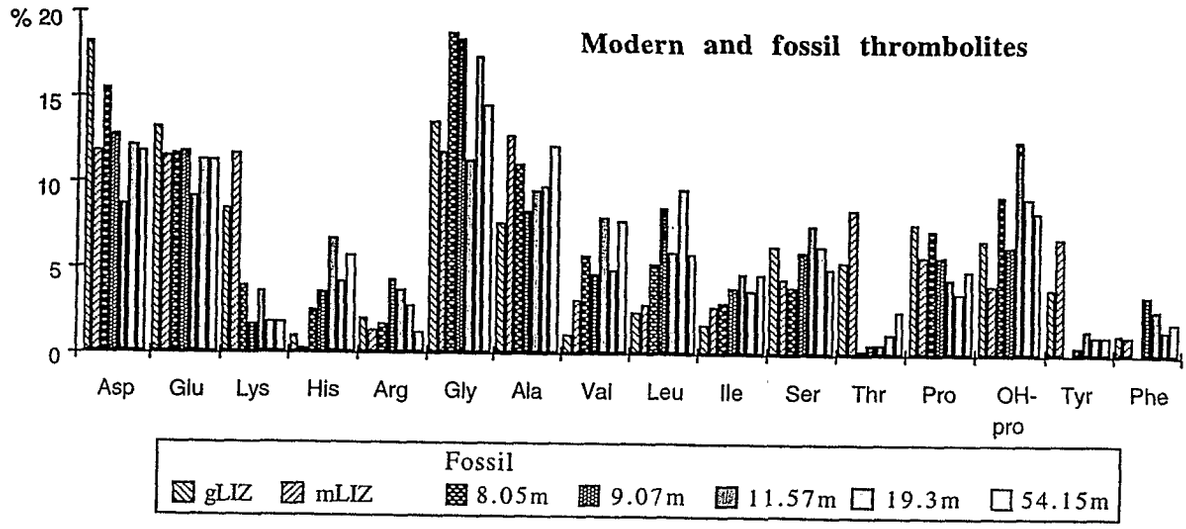

Fig. 15. Relative amino-acid composition of Tahiti Holocene thrombolitic fabrics compared to the modern ones from Lizard Island (GBR). *gLIZ* = growing part of thrombolite; *mLIZ* = mature part of a thrombolite. Major amino acids: *Asp* = aspartic acid; *Glu* = glutamic acid; *Ser* = serine; *Lys* = lysine; *His* = histidine; *Arg* = arginine; *Gly* = glycine; *Ala* = alanine.

tic and glutamic acids of 10–15%. These values are similar to those obtained on mature parts of microbialites from Lizard Island, but significantly lower than those from their growing surfaces and micrite in cavities (respectively, up to 20 and 32% aspartic acid; Reitner et al., 1995) (Fig. 15). The other characteristic of the Tahiti crusts is the abundance of hydroxyproline, which is a collagenous substance abundant in sponges and probably also in various cnidarians, including octocorals and hydrozoans. Its relative concentration, well above those reported in the Lizard Island microbialites (Reitner et al., 1995) (Fig. 15), indicate that metazoans may have proliferated in these microenvironments. These metazoans may have provided part of the initial organic substances, which could serve as the mineralizing matrix after recycling by microbial biofilms. The occurrence of hydroxyproline may be considered as characteristic of microbialites developed in environments dominated by metazoan–microorganism associations, because it is absent in deeper water microbialites (e.g. ledge rocks) (Fig. 16) where associated metazoans are rare or absent. It seems likely that where such metazoans are abundant, their degrading organic matter and their EPS are concentrated in zones where the organo-mineral interaction governing carbonate mineralization takes place.

The evidence for active participation of metazoans in the formation of Tahiti microbialites is indicated further by changes in concentration of aspartic acid, glycine and hydroxyproline between laminated crusts and thrombolites (Fig. 14). High glycine contents characterize thrombolitic facies, whereas greater amounts of aspartic acid and hydroxyproline occur in laminated crusts. This difference could reflect slight differences in the composition of organic matrices (especially organic tissues and metabolic products) and related mineralization processes between the two types of microbialites.

The apparent lack of typical microbial compounds in soluble organic matter does not imply that microbial organisms did not play a prominent role in microbialite accretion. The biochemical composition of microbial EPS is not well enough known to understand its participation in the composition of a complex organic matrix. However, we report here an as yet unidentified compound that may characterize carbonate mineralization mediated by microbial mucus. The presence of bacterial remains in the Tahiti crusts suggests that the microbes underwent also individual processes of biomineralization. The capacity of bacteria to concentrate Ca^{2+} and Mg^{2+} on, and around, their cells and to promote $CaCO_3$ precipitation has been demonstrated (e.g. Morita,

Fig. 16. SEM micrograph of microbialites from the Red Sea foreslopes (ledge rocks) showing an ultrastructure similar to that of the Tahiti microbialites and characterized by the great abundance of 0.1–0.2-μm-sized spherical to subspherical bodies closely packed in aggregates, grape-like clusters and swarms. Scale bar: 1 μm.

1980; Castanier, 1987). It is also known that microbial mucilage appears as "an ideal site for bacterial biomineralization" (Chafetz and Buczynski, 1992).

The occurrence of muramic and diaminopimelic acids, characterizing mureins of bacterial cell walls, in insoluble organic matrices suggests that bacteria played a role in transformation processes. These results are consistent with those obtained on mature portions of Lizard Island thrombolites, where a high proportion of non-proteinaceous amino acids, especially bacterial diaminopimelic acid, has been reported (Reitner et al., 1995). Therefore, it seems likely that the bacterial degradation of organic matter may have enhanced carbonate precipitation, related to the creation of a specific chemical environment via sulphate reduction and ammonification as it has been shown both in laboratory experiments and natural environments. Sulphate reduction is the predominant anaerobic pathway in reef interstitial waters (Tribble et al., 1990).

The two-layered system of the Tahiti microbialites and the related changes in microstructure, from dense to clotted or mottled micrites, may reflect slight differences in the composition of organic substrates that mediated calcification processes. A clotted or peloidal nature of micrites is common in many microbialites and is interpreted as in-place precipitation in organic mucilage (e.g. Monty, 1976; Riding, 1991; Camoin and Montaggioni, 1994). Presumably, this is due to enrichment in Ca-binding proteins where 0.1-μm-sized cryptocrystalline high-Mg calcite aggregates form the initial precipitation of a 'peloidal cement' (Reitner, 1993; Zankl, 1993; Reitner et al., 1995). Défarge et al. (1996) suggested

that peloidal nuclei in the freshwater stromatolites they studied are organo-minerals related to a three-dimensional polysaccharide network. On the other hand, it has been shown that peloids may also form via calcification of microbes (Castanier et al., 1989; Buczynski and Chafetz, 1991).

7. Environmental significance of microbialites in Tahiti reefs

It has been demonstrated that environmental conditions in Tahiti were optimal for reef development during the last 13,500 years, based on the ecological characteristics of biological associations, reef growth rates, $CaCO_3$ accumulation rates and geochemistry of coral skeletons (Camoin and Montaggioni, 1994; and this study). Reef growth rates averaged 7.9 mm yr^{-1} for the last 13,500 years at sites P7 and P8 (Montaggioni et al., 1997). Reef growth strategy cannot be determined for the *Porites nigrescens/P. lichen* assemblage recorded at the base of the cored reef sequence near the pass (P9 and P10) owing to the uncertainty of its palaeobathymetric significance. By contrast, coeval coralgal frameworks in the central part of the barrier reef complex (P7 and P8) were formed by a domal *Porites* association with a keep-up growth strategy (Fig. 3). The *Acropora* gr. *robusta/danai* association that occurred at all sites for more than 11,000 years (Fig. 3) indicates that, throughout this time span, reef frameworks developed continuously in a high-energy environment, at maximum water depths of 5–6 m, and that the barrier reef margin was able to keep pace with rising sea level (keep-up growth strategy).

In Tahiti reefs, microbialites developed directly on corals in growth position or, more commonly, over associated encrusting organisms (coralline algae, vermetid gastropods and crustose foraminifers). With the exception of a few serpulid worms, microbialites form generally the last stage of encrustation in an open cavity system with freely circulating normal-marine water, where they grew over dead parts of coral branches in cryptic niches, perhaps some distance within the reef framework. This implies that there was generally no direct space competition between coralgal communities and microbialites and that some time elapsed prior to the formation of the microbialites.

The widespread occurrence of microbialites throughout the Tahiti post-glacial reef sequence suggests that they were able to keep pace with reef accretion rates that ranged from 11 to 20.6 mm yr^{-1} (Montaggioni et al., 1997). Such accretion rates are well above those reported in ledge rocks and reef cave microbialites, which generally grow at rates of 3.5–10 $\mu m\ yr^{-1}$ (Brachert and Dullo, 1991) and 50–100 μm yr^{-1} (Reitner, 1993), respectively. However, the irregular vertical and areal distribution of microbialites in Tahitian reef cores suggests that their development may have been closely related to the prevailing environmental conditions.

In Tahiti reef cavities, the general sequence of the biota involving corals, encrusting organisms (mainly red algae and crustose foraminifers), borers (cyanobacteria, sponges, worms), microbial crusts and finally encrusters and borers (especially worms) probably developed in response to subtle changes in the ecological parameters within the interstices between adjacent coral colonies. A similar sequence was reported by Webb and Jell (1997) in Heron Island reefs. The inferred sequence was probably partly driven by decreases both in light and energy, related to a progressive burial by coral growth. The successive development of photophilic and sciaphilic organisms indicates that the decrease in illumination played a critical role in the time represented by the growth of the red algal crusts and microbial coatings over the coral branches. Serpulid worms that locally form the last stage of encrustation on the outer surfaces of microbialites indicate low light levels and are generally restricted to cryptic, shaded environments in protected areas (see Jones and Hunter, 1991; Martindale, 1992). At Discovery Bay, loosely stacked plates of *A. palmata* have photophilic encrusting organisms to depths of about 80 cm and sciaphilic organisms below that (Scoffin and Hendry, 1984). In shallow water caves of fringing reefs of Lizard Island, thick microbialite crusts (thrombolites) dominate in effective darkness (1–4 lx), while thick crusts of coralline algae develop in reduced light conditions (5–100 lx) and active coral growth occurs where light intensities are between 600 and 2000 lx at noon (Reitner et al., 1995). This lateral succession can easily be transferred to vertical successions representing a continuous decrease of light flux, in turn reflecting a transgressive event (Zankl,

1993; Reitner et al., 1995). By contrast, a similar biological succession reported in Pleistocene lagoonal deposits from the Grand Cayman was interpreted as being related to decreasing energy and light during regressive conditions (Jones and Hunter, 1991).

The dominance of laminated structures in large pores occurring in robust acroporid frameworks indicates that they were more light- (and possibly energy-) tolerant than the thrombolites. The latter formed in reduced light and energy conditions, in association with deeper coralgal associations and overgrowing laminated crusts in residual pores of shallower coralgal assemblages. These conclusions contrast with previous report of thrombolitic fabrics in high-energy conditions, whereas stromatolite-like structures characterize lower-energy conditions (Zankl, 1993).

Although it seems likely that most Quaternary and modern reef micritic microbialites developed in cryptic habitats with reduced light irradiance, we believe that the decreasing light conditions alone cannot account for their development in Quaternary reef tracts. Temporary periods of runoff, which brought terrigenous sediments (including weathered products with high Si, Fe and Al contents) to the reefs, may also have induced subtle fluctuations in ecological parameters, especially including an increase in nutrient availability and alkalinity of interstitial reef waters. A strong correlation between the abundance of microbialites and terrigenous influx is noted in the vicinity of Papeete Pass (P9 and P10) which corresponds to an ancient river outlet located in front of the modern Tipaerui River. Similar direct relationships between the abundance of microbialites and terrigenous influx were reported by Reitner (1993) in reef caves from Lizard Island, but similar crusts occur also in reefs far removed from siliciclastic sources (see Webb, 1996). Freshwater input probably slightly increased carbonate alkalinity from the weathering of basalts and soils inducing an increase in HCO_3 and CO_3^{2-} concentrations. Additionally, an increase in carbonate alkalinity may have been produced by organic decay processes. Increases in nutrient concentration favour algal settlement and, ultimately, microbial communities (see review by Hallock, 1988; Cuet et al., 1988; Montaggioni et al., 1993 for modern counterparts). River waters may contain up to ten times greater concentrations of nutrients (particularly Fe, P and N) than tropical sea surface waters (Livingstone, 1963). Similar concentrations are noted in freshwater lenses of various French Polynesian islands (Rougerie and Wauthy, 1993). It has been demonstrated that groundwater seepage may be a prominent process in modern fringing reefs (Marsh, 1977; D'Elia et al., 1981; Sansone et al., 1988). In agreement with studies emphasizing the importance of terrestrial groundwater seepage in nutrient input to coral reefs (e.g. Lewis, 1987), we assume that this may also have enriched reef interstitial waters in dissolved nutrients. Drilling operations in the lagoon of Papeete demonstrated the occurrence of groundwater in the basaltic basement and also in overlying detrital beds (Deneufbourg, 1971). Groundwater seepage was probably more active when sea level was significantly lower than nowadays and the reef located closer to the shore. It seems likely that nutrient concentrations may have decreased sharply when sea level reached a position high enough to limit the terrestrial input from weathering, groundwater seepage, and submergence of soils. The sharp decrease in microbialite abundance at 7 m.b.r.s. is dated at 5770 ± 100 ^{14}C yr B.P. and pre-dates slightly the stabilization of sea level at its present position (see also Pirazzoli and Montaggioni, 1988; Camoin and Montaggioni, 1994). Periodic inputs of nutrient-rich and more alkaline waters in the vicinity of the reef may have caused 'blooms' of microbial communities and of some metazoans, and enhanced $CaCO_3$ precipitation and calcification processes during the last 13,500 years. These changing physico-chemical conditions may have induced temporary stressful phases for reef communities but did not significantly affect overall reef growth. Because nutrients are rapidly taken up and incorporated by microbial organisms, the dissolved-nutrient levels may have remained low in surface waters and therefore did not significantly affect coral growth.

Reef interstitial water chemistry shows clear deviations from surface seawater, especially with elevated contents in inorganic nutrients (ammonia, phosphate, silicate), either due to the oxidation of organic matter in the reef framework (Tribble et al., 1990) or to large supply of nutrients via active upwelling of organic-rich fluids throughout the reef framework (Rougerie and Wauthy, 1993). Such upward circulation has been demonstrated in the Tahiti

P7 core and is also thought to account for increased alkalinity (Rougerie et al., 1997). Furthermore, nutrient levels may have increased sharply during last deglaciation events as a result of more intense circulation and upwelling, as suggested for the northern Great Barrier Reef (Marshall and Davies, 1988). Their impact on the development of Lizard Island microbialites was not considered (Reitner, 1993).

As a conclusion, the presented data, the available literature and the authors' personal experience, suggest that the key prerequisite for the development of microbialites in cryptic niches of Quaternary reefs consists of environmental perturbation involving parameters such as nutrient content, alkalinity and decreasing light and energy conditions. The data presented herein suggest that, during the last postglacial marine transgression, such conditions may have especially occurred when fringing reefs were directly exposed to land runoff and terrestrial groundwater seepage. These environmental conditions disappeared progressively with the upward decrease in terrigenous input throughout the postglacial reef sequence as a result of the landward shift of accumulation zones, related to sea level rise and the subsequent development of a lagoonal zone which acted as a sediment trap (Fig. 17). The development of microbialites in the cryptic niches of the reef framework ceased about 6000 years ago when the sea level approached its present position.

8. Summary and conclusions

Five drill cores from the barrier reef-edge of Tahiti afford the opportunity to document the widespread development of microbialites in an open cavity system with freely circulating normal-marine water that developed in the reef framework continuously from 13,500 to 6000 yrs B.P.

(1) Depending on the palaeotopography of the volcanic substrate, the base of the reef sequence includes assemblages of either branching *Porites* colonies, indicating a quiet-water environment (6–30 m) environment, or of domal *Porites* mixed with tabular acroporids and gracile branching red algae, characterizing an outer slope to reef flat (5–15 m deep) environment. The overlying reef framework is composed predominantly of a robust-branching community, an *Acropora* gr. *danai/robusta* assemblage, heavily encrusted by coralline algae and sessile vermetid gastropods, which typifies high-energy reef edges and upper reef slopes in water less than 6 m deep.

(2) Microbial crusts generally form the last stage of encrustation of coral colonies, or more commonly of associated encrusting organisms. In most cored reef sections, microbialites appear as a major structural and volumetric component of Tahiti reefs and may locally form 80% of the rock. They include laminated crusts and clotted micritic masses, commonly associated in compound crusts, that probably reflect differences in the composition of the involved biological communities and/or the biomineralization processes that controlled the accretion of the crusts. The crust types are also differentiated on the basis of their biochemical composition. The scarcity of extraneous particles in the Tahiti crusts suggests that sediment trapping was much less important than calcification of organic mucilage associated with living or decaying organisms and in-place, microbially mediated, precipitation of micrite.

The isotopic composition of the microbialites (+2.05 to +3.92‰ $\delta^{13}C$, and −0.86 to +0.86‰ $\delta^{18}O$) is typical for a non-enzymatic fractionation close to that expected for calcitic cements precipitated at equilibrium with normal seawater.

Proteinaceous compounds are abundant, with relative concentrations in aspartic and glutamic acids of 10–15%; the abundance of hydroxyproline indicates that metazoans may have proliferated in these microenvironments and represent the initial source of organic substrates that were mineralized during recycling by microbial biofilms. Microbial organisms (especially bacteria and possible nannobacteria) seemingly played a major role in transformation processes and in carbonate precipitation via the bacterial degradation of organic matter; they also underwent individual processes of biomineralization.

(3) The nature of the biological communities involved, geochemical data, and reef accretion and high calcification rates, imply that local environmental conditions were optimal for reef growth for the last 13,500 years. Besides the overall decrease in light and energy conditions reflecting progressive burial by coral growth, the widespread development of microbialites within the reef framework

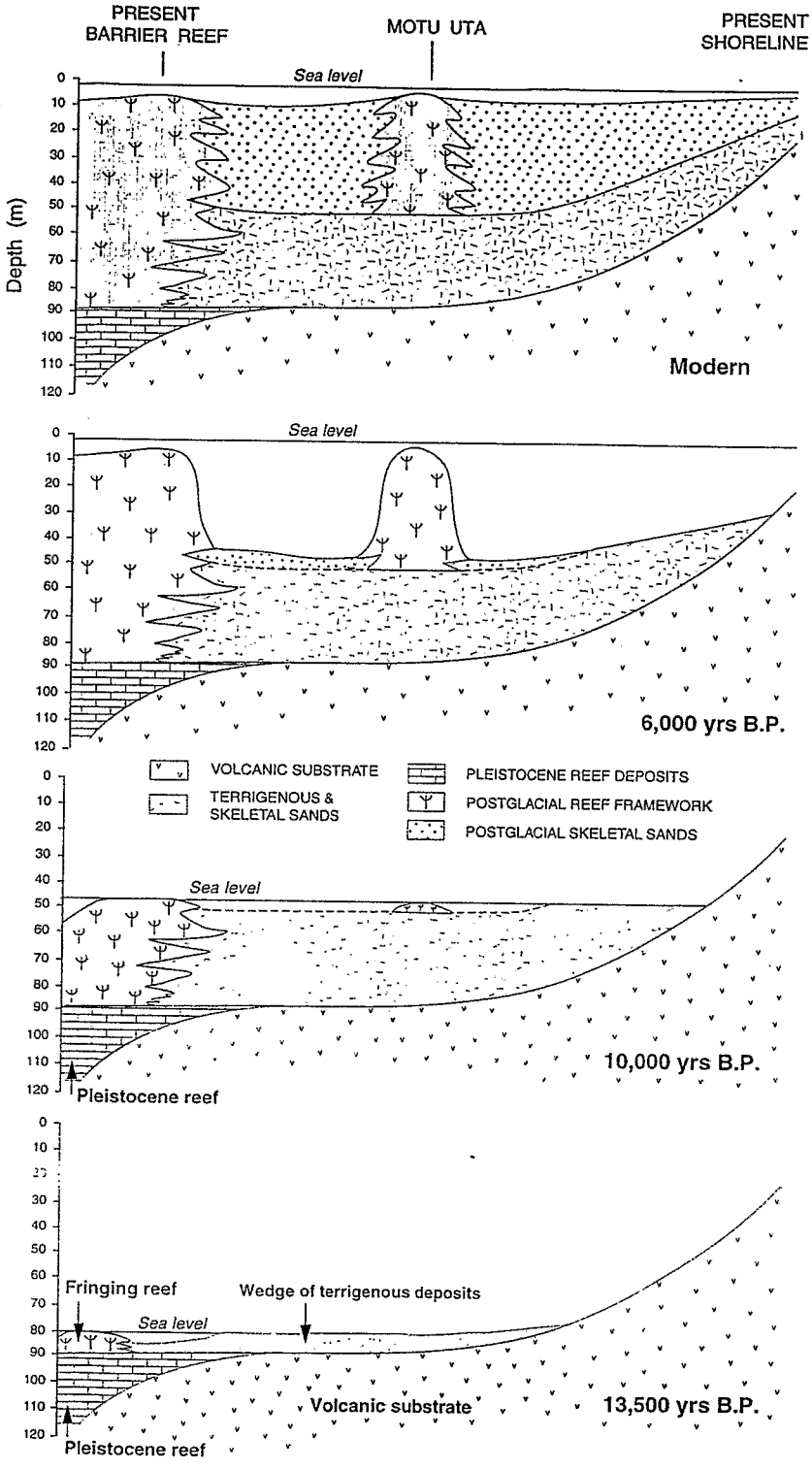

Fig. 17. Stages of reef development over the last 13,500 years.

may be related to increased alkalinity and nutrient availability in interstitial waters owing to terrestrial groundwater seepage and periodic runoff events. The development of microbialites in the cryptic niches of the reef framework ceased about 6000 years ago, when the sea level approached its present position.

(4) Microbial communities have played a more prominent role in Quaternary reef tracts than previously recognized, especially in the strengthening of coralgal frameworks due to their rapid lithification. We agree with Riding (1991) that the peloidal thrombolitic fabrics in Recent reefs may be examples of microbial carbonates surviving to modern times in favourable habitats, but in a form which has tended to be overlooked. Furthermore, we believe that these microbialites are analogs of the lithified micritic crusts that characterize many Phanerozoic buildups (see the review by Webb, 1996).

Acknowledgements

We thank the Programme National Récifs Coralliens (PNRCO) and ORSTOM (especially F. Rougerie and J. Récy) for the financial and logistical support; the past Director of ORSTOM-Tahiti, Mr. Boccas, the ORSTOM drillers from Nouméa, Y. Join, C. Ihilly and J.L. Laurent, for their efficient work, and the Director of the Papeete harbour who authorized the drilling operations. We are indebted to Brian Pratt and Gregg Webb for their reviews and valuable comments that improved the paper. Thanks also to Colin Braithwaite, Ian Macintyre and Joachim Reitner who reviewed an earlier draft of the manuscript. The isotope and trace element analyses were carried out at the Laboratoire de Géologie des Bassins Sédimentaires (Université P. and M. Curie, Paris; Dir. Pr M. Renard) by M. Colonna, E. Biger and G. Richebois, and at the Department of Paleontology of the University of Erlangen (Germany) by M. Joachimski.

References

Adey, W.H., 1986. Coralline algae as indicators of sea level. In: Van de Plassche, O. (Ed.), Sea-Level Research, A Manual for the Collection and Evaluation of Data. Geo-Books, Norwich, pp. 229–280.

Aissaoui, D., 1988. Magnesian calcite cements and their diagenesis: dissolution and dolomitization. Sedimentology 35, 821–841.

Bard, E., Hamelin, B., Arnold, M., Montaggioni, L.F., Cabioch, G., Faure, G., Rougerie, F., 1996. Deglacial sea level record from Tahiti corals and the timing of global meltwater discharge. Nature 382, 241–244.

Bouchon, C., 1996. Recherches sur des peuplements de scléractiniaires indo-pacifiques (Mer Rouge, Océan Indien, Océan Pacifique). Thèse Doct.-ès Sci. Marseille, Univ. Aix-Marseille II, 306 pp.

Brachert, T.C., 1994. Palaeocecology of enigmatic tube microfossils forming 'cryptalgal' fabrics (Late Quaternary, Red Sea). Palaeontol. Z. 68, 299–312.

Brachert, T.C., Dullo, W.Chr., 1991. Laminar micrite crusts and associated foreslope processes, Red Sea. J. Sediment. Petrol. 61, 354–363.

Buczynski, C., Chafetz, H.S., 1991. Habit of bacterially induced precipitates of calcium carbonate and the influence of medium viscosity on mineralogy. J. Sediment. Petrol. 61, 226–233.

Burne, R.V., Moore, L.S., 1987. Microbialites: organosedimentary deposits of benthic microbial communities. Palaios 2, 241–254.

Cabioch, G., Taylor, F.W., Recy, J., Edwards, R.L., Gray, S.C., Faure, G., Burr, G.S., Correge, T., 1998. Environmental and tectonic influences on growth and internal structure of a fringing reef at Tasmaloum (South West Espiritu Santo, New Hebrides Island Arc, South West Pacific). In: Camoin, G., Davies, P.J. (Eds.), Reefs and Carbonate Platforms of the Pacific and Indian Ocean. Spec. Publ. Int. Assoc. Sedimentol. 25, 261–277.

Cabioch, G., Camoin, G.F., Montaggioni, L.F., Faure, G., 1999. Postglacial growth history of a French Polynesian barrier reef, Tahiti, central Pacific. Sedimentology (in press).

Camoin, G.F., Montaggioni, L.F., 1994. High energy coralgal-stromatolite frameworks from Holocene reefs (Tahiti, French Polynesia). Sedimentology 41, 655–676.

Camoin, G.F., Colonna, M., Montaggioni, L.F., Casanova, J., Faure, G., Thomassin, B.A., 1997. Holocene sea level changes and reef development in southwestern Indian Ocean. Coral Reefs 16, 247–259.

Castanier, S., 1987. Microbiogéologie: processus et modalités de la carbonatogenèse bactérienne. Thèse Doct. ès-Sci., Univ. Nancy, 511 pp.

Castanier, S., Maurin, A., Perthuisot, J.-P., 1989. Production expérimentale de corpuscules carbonatés sphéroïdaux à structure fibro-radiaire. Réflexion sur la définition des oolides. Bull. Soc. Géol. Fr. 5, 589–595.

Chafetz, H.S., Buczynski, C., 1992. Bacterially induced lithification of microbial mats. Palaios 7, 277–293.

Chevalier, J.P., 1978. Les coraux des Iles Marquises. Cah. Pac. 21, 243–283.

Cuet, P., Naim, O., Faure, G., Conan, J.Y., 1988. Nutrient-rich groundwater impact on benthic communities of La Saline fringing reef (Reunion Island, Indian Ocean): preliminary re-

sults. Proc. 6th Int. Coral Reef Symp., Townsville 2, pp. 207–212.

Défarge, C., Trichet, J., Jaunet, A.-M., Robert, M., Tribble, J., Sansone, F.J., 1996. Texture of microbial sediments revealed by cryo-scanning electron microscopy. J. Sediment. Res. 66, 935–947.

Déjardin, P., 1996. Etude d'un géosystème récifal insulaire (récif barrière de Tahiti, Polynésie Française). Caractérisation géochimique des différents compartiments et de leurs interactions. Thèse. Doct. Univ. L. Pasteur, Strasbourg, 167 pp.

Delesalle, B., Galzin, R., Salvat, B., 1985. French Polynesian coral reefs. Proc. 5th Int. Coral Reef Congr. 1.

D'Elia, C.F., Webb, K.L., Porter, J.W., 1981. Nitrate-rich groundwater inputs to Discovery Bay, Jamaica: a significant source of N to local reefs. Bull. Mar. Sci. 31, 903–910.

Deneufbourg, G., 1971. Etude géologique du Port de Papeete, Tahiti, Polynésie Française. Cah. Pac. 15, 75–82.

De Ridder, C., 1986. Echinides. In: Guille, A. (Ed.), Guide des étoiles de mer, oursins et autres échinodermes du lagon de Nouvelle Calédonie. Off. Rech. Sci., Tech. Outre-Mer (ORSTOM), Paris, 53 pp.

Dill, R.F., Shinn, E.A., Jones, A.T., Kelly, K., Steinen, R.P., 1986. Giant subtidal stromatolites forming in normal salinity waters. Nature 324, 55–58.

Done, T.J., 1982. Patterns in the distribution of coral communities across the central Great Barrier reef. Coral Reefs 1, 95–107.

Dravis, J.J., 1983. Hardened subtidal stromatolites, Bahamas. Science 219, 385–386.

Dullo, W.-Ch., Camoin, G.F., Blomeier, D., Casanova, J., Colonna, M., Eisenhauer, A., Faure, G., Thomassin, B.A., 1998. Sediments and sea level changes of the foreslopes of Mayotte, Comoro islands: direct observations from submersible. In: Camoin, G., Davies, P.J. (Eds.), Reefs and Carbonate Platforms of the Pacific and Indian Ocean. Spec. Publ. Int. Assoc. Sedimentol. 25, 219–236.

Faure, G., 1982. Recherches sur les peuplements de scléractiniaires des récifs coralliens de l'archipel des Mascareignes (Océan Indien occidental). Thèse Doct.-ès Sci. Univ. Aix-Marseille II, Marseille, 206 pp.

Faure, G., Laboute, P., 1984. L'atoll de Tikehau, Premiers résultats: Formations récifales, I: définition des unités récifales et distibution des principaux peuplements de scléractiniares. ORSTOM, Paris, Notes Doc. 22, pp. 108–136.

Folk, R.N., 1993. SEM imaging of bacteria and nannobacteria in carbonate sediments and rocks. J. Sediment. Petrol. 63, 990–999.

Folk, R.N., Land, L.S., 1975. Mg/Ca ratio and salinity: two control over crystallization of dolomite. Am. Assoc. Pet. Geol. Bull. 59, 60–68.

Gournay, J., Kirkland, B.L., Folk, R.L., Lynch, F.L., 1999. Evidence for nannobacterially precipitated dolomite in Pennsylvanian rocks, Utah. Sediment. Geol. 126, 243–252 (this issue).

Guo, L., Riding, R., 1994. Origin and diagenesis of Quaternary travertine shrub fabrics, Rapolano Terme, central Italy. Sedimentology 41, 499–520.

Hallock, P., 1988. The role of nutrient availability in bioerosion: consequences to carbonate buildups. Palaeogeogr., Palaeoclimatol., Palaeoecol. 63, 275–291.

Hardie, L., 1987. Dolomitisation: a critical view of some current views. J. Sediment. Petrol. 57, 166–183.

James, N.P., Ginsburg, R.N., 1979. The seaward margin of Belize barrier and atoll reefs. Spec. Publ. Int. Assoc. Sedimentol. 3, 191 pp.

Jones, B., Hunter, I.G., 1991. Corals to rhodolites to microbialites — a community replacement sequence indicative of regressive conditions. Palaios 6, 54–66.

Krumbein, W.E., 1979. Photolithotropic and chemoorganotrophic activity of bacteria and algae as related to beachrock formation and degradation (Gulf of Aqaba, Sinai). Geomicrobiol. J. 1, 139–203.

Kuhlman, D.H.H., Chevalier, J.-P., 1986. Les coraux (Scléractiniaires et Hydrocoralliaires) de l'atoll de Takapoto, îles Tuamotu: aspects écologiques. Mar. Ecol. 7, 75–104.

Land, L.S., Goreau, T.F., 1970. Submarine lithification of Jamaican reefs. J. Sediment. Petrol. 40, 457–462.

Land, L.S., Moore, C.H., 1980. Lithification, micritization and syndepositional diagenesis of biolithites on the Jamaican island slope. J. Sediment. Petrol. 50, 357–370.

Le Roy, I., 1994. Evolution des volcans en système de point chaud: île de Tahiti, archipel de la Société (Polynésie Française). Thèse Doct. Univ. Paris-Sud, Orsay, 271 pp.

Lewis, J.B., 1987. Measurements of groundwater seepage flux onto a coral reef: spatial and temporal variations. Limnol. Oceanogr. 32, 1165–1169.

Livingstone, D.A., 1963. Data of geochemistry, Chapter G.: composition of rivers and lakes. U.S. Geol. Surv. Prof. Pap. 440-G, 64 pp.

Macintyre, I.G., 1984. Extensive submarine lithification in a cave in the Belize Barrier Reef Platform. J. Sediment. Petrol. 54, 221–235.

Macintyre, I.G., Marshall, J.F., 1988. Submarine lithification in coral reefs: some facts and misconceptions. Proc. 6th Int. Coral Reef Symp., Townsville 1, pp. 263–272.

Macintyre, I.G., Reid, R.P., Steneck, R.S., 1996. Growth history of stromatolites in a Holocene fringing reef, Stocking Island, Bahamas. J. Sediment. Res. 66, 231–242.

Marsh, J.A., 1977. Terrestrial inputs of nitrogen and phosphorus on fringing reefs of Guam. Proc. 3rd Int. Coral Reef Symp., Miami 1, pp. 331–336.

Marshall, J.F., 1983. Submarine cementation within a high-energy platform reef: One Tree Reef, southern Great Barrier Reef. J. Sediment. Petrol. 53, 1133–1149.

Marshall, J.F., 1986. Regional distribution of submarine cements within a epicontinental reef system: central Great Barrier Reef. In: Schroeder, J.H., Purser, B.H. (Eds.), Reef Diagenesis. Springer, Berlin, pp. 8–26.

Marshall, J.F., Davies, P.J., 1988. *Halimeda* bioherms of the northern Great Barrier Reef. Coral Reefs 6, 139–148.

Martindale, W., 1992. Calcified epibionts as palaeoecological tools: examples from the Recent and Pleistocene reefs of Barbados. Coral Reefs 11, 167–177.

Montaggioni, L.F., 1988. Holocene reef growth history in mid-

plate high volcanic islands. Proc. 6th Int. Coral Reef Symp., Australia 3, pp. 455–460.
Montaggioni, L.F., Camoin, G.F., 1993. Stromatolites associated with coralgal communities in Holocene high-energy reefs. Geology 21, 149–152.
Montaggioni, L.F., Cuet, P., Naim, O., 1993. Effect of nutrient excess on a modern fringing reef (Réunion Island), Western Indian Ocean, geological implications. In: Ginsburg, R.N. (Ed.), Global Aspects of Coral Reefs, Case Histories. Univ. Miami, FL, pp. N27–N33.
Montaggioni, L.F., Cabioch, G., Camoin, G.F., Bard, E., Ribaud, A., Faure, G., Déjardin, P., Récy, J., 1997. Continuous record of reef growth over the past 14 k.y. on the mid-Pacific island of Tahiti. Geology 25, 555–558.
Monty, C.L.V., 1976. The origin and development of cryptalgal fabrics. In: Walter M.R. (Ed.), Stromatolites. Dev. Sedimentol. 29, 193–249.
Moore, C.H., Graham, E.A., Land, L.S., 1976. Sediment transport and dispersal across the deep fore-reef and Island slope (−55 m to −305 m), Discovery Bay, Jamaica. J. Sediment. Petrol. 46, 174–187.
Morita, R.Y., 1980. Calcite precipitation by marine bacteria. Geomicrobiol. J. 2, 63–82.
Morita, R.Y., 1988. Bioavailability of energy and starvation survival in nature. Can. J. Geomicrobiol. 34, 436–441.
Pedone, V., Folk, R.L., 1996. Formation of aragonite cements by nannobacteria in the Great Salt Lake, Utah. Geology 24, 763–765.
Pirazzoli, P.A., Montaggioni, L.F., 1988. The 7000 years sea level curve in French Polynesia: geodynamic implications for mid-plate volcanic islands. Proc. 6th Int. Coral Reef Symp., Townsville 3, pp. 467–472.
Reid, R.P., Browne, K.M., 1991. Intertidal stromatolites in a fringing Holocene reef complex in the Bahamas. Geology 19, 15–18.
Reid, R.P., Macintyre, I.G., Browne, K.M., Steneck, R.S., Miller, T., 1995. Modern marine stromatolites in the Exuma Cays, Bahamas: uncommonly common. Facies 33, 1–18.
Reitner, J., 1993. Modern cryptic microbialite/metazoan facies from Lizard Island (Great Barrier Reef, Australia), formation and concepts. Facies 29, 3–40.
Reitner, J., Gautret, P., Marin, F., Neuweiler, F., 1995. Automicrites in a modern microbialite. Formation model via organic matrices (Lizard Island, Great Barrier Reef, Australia). Bull. Inst. Océanogr. Monaco 14, 237–263.
Riding, R., 1991. Classification of microbial carbonates. In: Riding, R. (Ed.), Calcareous Algae and Stromatolites. Springer, Berlin, pp. 55–87.
Rougerie, F., Wauthy, B., 1993. The endo-upwelling concept: from geothermal convection to reef construction. Coral Reefs 12, 19–30.
Rougerie, F., Fichez, R., Harris, P., Andrié, C., 1997. The Tahiti barrier reef: a reservoir for inorganic and organic nutrients. Proc. 8th Int. Coral Reef Symp., Panama 2, pp. 2059–2062.
Sansone, F.J., Andrews, C.C., Buddemeier, R.W., Tribble, G.W., 1988. Well-point sampling of reef interstitial water. Coral Reefs 7, 19–22.
Scoffin, T.P., Hendry, M.D., 1984. Shallow-water sclerosponges on Jamaican reefs and a criterion for recognition of hurricane deposits. Nature 307, 728–729.
Tribble, G.W., Sansone, F.J., Smith, S.V., 1990. Stoichiometric model of carbon diagenesis within a coral reef framework. Geochim. Cosmochim. Acta 54, 2439–2449.
Vasconcelos, C., McKenzie, J.A., 1997. Microbial mediation of modern dolomite precipitation and diagenesis under anoxic conditions (Lagoa Vermelha, Rio de Janeiro, Brazil). J. Sediment. Res. 67, 378–390.
Veron, J.E.N., 1986. Corals of Australia and the Indo-Pacific. Angus and Robertson, London, 644 pp.
Webb, G.E., 1996. Was Phanerozoic reef history controlled by the distribution of non-enzymatically secreted reef carbonates (microbial carbonate and biologically induced cement). Sedimentology 43, 947–971.
Webb, G.E., Jell, J.S., 1997. Cryptic microbialite in subtidal reef framework and intertidal solution cavities in beachrock, Heron Reef, Great Barrier Reef, Australia: preliminary observations. Facies 36, 219–223.
Webb, G.E., Baker, J.C., Jell, J.S., 1998. Inferred syngenetic textural evolution in Holocene cryptic reefal microbialites, Heron Reef, Great Barrier Reef, Australia. Geology 26, 355–358.
Weiner, S., Traub, W., Lowenstam, H.A., 1983. Organic matrix in calcified exoskeletons. In: Westbroeck, P., De Jong, E.W. (Eds.), Biomineralization and Biological Metal Accumulation. Reidel, Dordrecht, pp. 204–224.
Zankl, H., 1993. The origin of high-Mg calcite microbialites in cryptic habitats of Caribbean coral reefs — their dependence on light and turbulence. Facies 29, 55–60.

Apports de la croissance des coraux à l'étude sismo-tectonique de Futuna (territoire de Wallis et Futuna, Pacifique Sud-Ouest)

Data provided by coral growth for sismotectonic studies in Futuna (French Overseas Territory of Wallis and Futuna, southwest Pacific)

Guy Cabioch, Stéphane Calmant, Robert Pillet, Bernard Pelletier, Marc Régnier, Pierre Lebellegard

Laboratoire de géologie et géophysique, UMR « Géosciences Azur » 6526, centre IRD de Nouméa, BP A5, 98848 Nouméa cedex, Nouvelle-Calédonie

(Reçu le 5 avril 1999, accepté après révision le 19 juillet 1999)

Abstract — The morphology and growth analysis of coral microatolls using X-rays indicates that after a subsidence of 3 cm from 1977 to 1993, an uplift of 5 cm occurred in 1993 in the southeast of Futuna (southwest Pacific). These vertical motions are related to the strain accumulation followed by their relaxation during the earthquake (Mw: 6.4) on 12 March 1993. The locations published by the global network are not in agreement with the aftershocks recorded locally and the co-seismic uplifts observed on the reefs. The latter indicate instead that the rupture area is located below the southwest of Futuna at an average depth of 8 km. (© 1999 Académie des sciences / Éditions scientifiques et médicales Elsevier SAS.)

corals / microatolls / vertical motions / seismicity / Futuna / France

Résumé — L'analyse de la morphologie et de la croissance des microatolls coralliens par radiographie X indique, qu'après une subsidence de 3 cm de 1977 à 1993, une surrection de 5 cm a eu lieu en 1993, au sud-est de Futuna (Pacifique sud-ouest). Ces mouvements verticaux sont associés à l'accumulation des contraintes et à leur relaxation lors du séisme (Mw : 6,4) du 12 mars 1993. Les différentes localisations publiées pour ce séisme par le réseau mondial ne s'accordent, ni avec les répliques enregistrées localement, ni avec les surrections cosismiques observées. Celles-ci permettent, en revanche, de localiser la zone de rupture sous la pointe sud-ouest de Futuna, à une profondeur moyenne de 8 km. (© 1999 Académie des sciences / Éditions scientifiques et médicales Elsevier SAS.)

coraux / microatolls / mouvements verticaux / séismes / Futuna / Futuna

Abridged version

Introduction

The islands of Futuna and Alofi (French Overseas Territory of Wallis and Futuna, southwest Pacific) are the emerged part of the Horn submarine ridge. This ridge is located at the junction of the North Fiji basin and the Lau basin, south of the Vitiaz fossil lineament and north of the North Fiji fracture zone, a major transform segment of the Australian-Pacific plate boundary (Pelletier et al., 1998) (*figure 1A*). These islands are made up of a succession of submarine volcanic products deposited during the Late Pliocene. The nature of this volcanic material indicates a shift from a convergent regime (suduction

Note présentée par Jacques Angelier.

* Correspondance et tirés à part.
cabioch@noumea.ird.nc

of the Vitiaz-Tonga) to a transform regime (North Fiji fracture zone) (Grzesczyk et al., 1987; 1991). A series of reef terraces, presumably Quaternary in age, ranges from the present sea surface to an altitude reaching 400 m (Grzesczyk et al., 1989).

Seismic swarms commonly occurred around the islands of Futuna and Alofi occasionally accompanied by tsunamis (Louat et al., 1989; Monzier et al., 1993; Régnier, 1994). The most recent strong earthquakes felt in Futuna were those of 23 March 1977 (Mw: 6.3), 27 March 1986 (Mw: 6.0) and 12 March 1993 (Mw: 6.4). This last one (centroid epicentre given at 14.248° S. 178.298° W, focal depth 'normal' unspecified, *figure 1B*) caused several landslides, a tsunami, an uplift of several centimetres of the reef flat in the south and southwest parts of the island of Futuna, much building damage and the death of 3 people (Monzier et al., 1993; Régnier, 1994). An uplift of several tens of centimeters was observed on the modern coral reefs in the Léava area (Monzier et al., 1993) (*figure 1B*). At this time, no data are available for the reef terrace ages, the Quaternary uplift rate of the islands, the historical seismicity and the recurrence of the large destructive earthquakes.

In order to study the tsunamic and seismic hazards in Futuna, a program including sismology, geodesy and neotectonics, funded by PNRN (*Programme National français sur les Risques Naturels*), is in progress. The aim of this paper is to present some results gained during our first field trip in 1998: we give herein data obtained by the growth analysis of the coral microatolls observed on the modern reef flats, which yields useful indications on the pre- and co-seismic vertical motions associated with the 1993 earthquake.

Field data

On the reefs, the corals are distributed from the top of the reef flat, just below the sea surface, to several tens of meters of depth, along the reef slope. The corals living just below the present sea surface can give valuable information on the amount of co-seismic uplift by observations of the dead (emerged) and the living (still submerged) parts of corals (Knutson et al., 1972; Taylor et al., 1982). The analysis of the coral morphology and the sclerochronological study by examination of X-ray radiographies provide data on the trend of the growth axes and the pattern of coral growth, then on the small variations due to co-seismic uplifts (Knutson et al., 1972; Taylor et al., 1982; Woodroffe and McLean, 1990).

Such studies were conducted along the south coast of Futuna. We recognized several coral colonies, belonging to *Porites* species, at the back of the reef flat in the area of Vélé (*figure 1B*). These coral colonies show a typical microatoll morphology (sensu Stoddart and Scoffin, 1979) in relation to recent relative sea level variations due to uplift or submergence. We examined the morphology of these colonies and X-ray radiographs of slabs (an example of radiography is given in *figure 2*), which indicates several periods of perturbation in the coral growth (*figure 3*). By counting the annual growth bands, we identify a break of the coral growth in 1977 probably due to a co-seismic uplift (noted 1 in *figure 3*). From this date, the growth axis direction became more or less vertical, suggesting a progessive submergence of the colony (noted 2 in *figure 3*). The vertical growth is suddenly interrupted in 1993 by a co-seismic uplift, and the growth trend became horizontal (noted 3 in *figure 3*). The observed uplift is 5 cm. It is noteworthy that the reef flat is not recovered by fine sands which could be fatal for the coral colonies.

Discussion

The epicentre of the 1993 earthquake given by the global network is located, according to the available catalogues, at about 15 km westward (Centroid Moment Tensor Solution, CMTS) or southwestward (NEIC) from Futuna (*figure 1B*). However, aftershocks recorded no later than two days after the main shock are located below the southern part of Futuna at shallow depths (Régnier, 1994). This result suggests that the main earthquake was probably superficial and very close to the island of Futuna. This hypothesis is supported by the amount of the observed uplifts on the reef flats. Using the location and the solution given by the CMT catalogue (CMTS epicentre, size = 20 × 10 km, slip = 0.7 m), the simulated uplift (according to the dislocation model of Okada, 1985) is much lower than observed along the south coast of Futuna. In order to obtain the best fit with field observations, we modify the location of the ruptured fault (*figure 4*). The best fit corresponds to a shallow rupture located very close to the south west part of Futuna (178.15°W and 14.30°S and at a depth of 8 km), inducing an uplift of 20 cm in Léava and 5 cm in Vélé (*figure 4*). According to the depth found, the rupture may have reached the surface. This is in agreement with the occurrence of a tsunami along the south and southwest coasts of Futuna and the sound waves heard by the inhabitants.

A simulation of the evolution of the vertical motion at Vélé is shown in *figure 5*. This simulation is based on the dislocation model (Okada, 1985) for increasing strain release, that is for slip and ruptured fault increasing with time. According to this simulation, the deformation, which is equal and opposite to the co-seismic displacement, does not linearly increase with time. The microatoll morphology indicates that between 1977 and 1993, the *Porites* grew upward (3 cm ± 2 mm). Considering that the later value corresponds to the amplitude of the subsidence during this period, we obtain that the lack of slip was 52 ± 2 cm in 1977 (*figure 5*). The accumulation rate of the lack of slip would be (70–52) (1993–1977) = 1.1 cm·yr^{-1} (± 0.2 cm·yr^{-1}) and the duration of strain accumulation was 70/1.1 = 64 ± 12 yr until the seismic rupture.

Conclusion

The analysis of the coral growth of microatolls living just below the present-day sea surface along the south coast of Futuna gives useful indications on the occurrence and amplitudes of the recent vertical motions. Corals provide data for the study of seismic hazards when historical seismological data are missing. This first study provides new information on the 1993 Futuna earthquake. Vertical motion recorded by coral colonies allows precise location of the ruptured area and suggests interseismic strain accumulation.

1. Introduction

Les îles de Futuna et d'Alofi (territoire français d'Outre-Mer de Wallis et Futuna), formant la partie émergée de la ride sous-marine de Horne, sont situées à la jonction entre les bassins Nord-Fidjien et de Lau, au sud du linéament fossile du Vitiaz et au nord immédiat de la zone de fracture Nord-Fidjienne, une zone transformante majeure de la frontière actuelle entre les plaques Pacifique et Australie (Pelletier et al., 1998) (*figure 1A*). Elles sont composées de formations volcaniques sous-marines superposées, d'âge Pliocène supérieur à terminal, témoignant du passage d'un régime convergent (subduction du Vitiaz–Tonga) à transformant (zone de fracture Nord-Fidjienne) (Grzesczyk et al., 1987 ; 1991). Elles présentent également de nombreuses terrasses récifales culminant à une altitude de 400 m, dont l'âge est supposé Quaternaire (Grzesczyk et al., 1989).

Les îles de Futuna et d'Alofi sont régulièrement soumises à des crises sismiques, parfois accompagnées de raz de marée (Louat et al., 1989 ; Monzier et al., 1993 ; Régnier, 1994). Les séismes récents les plus significatifs ont été ceux du 23 mars 1977 (Mw : 6,3), du 27 mars 1986 (Mw : 6,0) et du 12 mars 1993 (Mw : 6,4). Ce dernier (épicentre centroïde donné à 14,248°S, 178,298°W, profondeur focale « normale » non résolue) a provoqué de très nombreux glissements de terrain, un petit raz de marée, la surrection de quelques centimètres à plusieurs dizaines de centimètres du platier corallien de la partie sud et sud-ouest de l'île, de nombreux dégâts matériels et la mort de 3 personnes (Monzier et al., 1993 ; Régnier, 1994). Les surrections cosismiques associées à ce séisme ont été maximales au niveau du récif frangeant de Léava

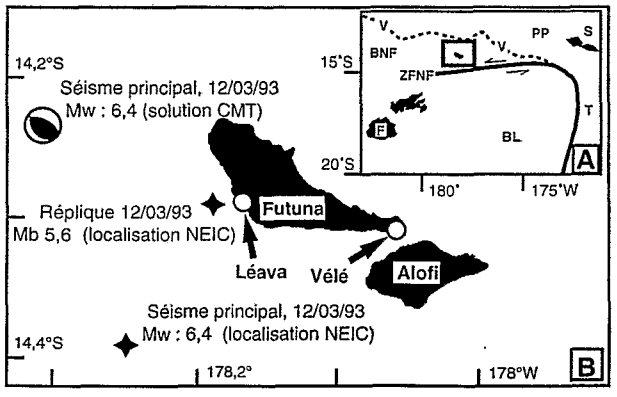

Figure 1. Les îles de Futuna et Alofi. A. Leur situation dans le contexte régional du Pacifique Sud-Ouest. Bassin Nord-Fidjien : BNF ; bassin de Lau : BL ; linéament fossile du Vitiaz : V ; Fidji : F ; Samoa : S, plaque Pacifique : PP. Le trait épais souligne la zone de fracture Nord-Fidjienne (ZFNF) et la fosse de Tonga (T). B. Localisation des sites d'étude et des séismes de la crise de mars 1993.

The islands of Futuna and Alofi. **A.** Their location in the southwest Pacific. North Fiji Basin: BNF; Lau Basin: BL; Vitiaz fossil lineament: V; Fiji: F; Samoa: S; Pacific Plate: PP. The thick line represents the North Fiji fracture zone (ZFNF) and the Tonga trench (T). **B.** Location of the studied sites and epicentres of the major events of the March 1993 seismic crisis.

(*figure 1B*). À ce jour, nous ne possédons aucune donnée sur l'âge des terrasses, le taux de surrection des îles, la séismicité historique et la récurrence des séismes destructeurs.

Nous réalisons un programme d'étude regroupant sismologie, géodésie et néotectonique, portant sur l'aléa sismique et tsunamique à Futuna. Ce programme est financé par le PNRN (Programme national sur les risques naturels). Cette note a pour objectif de présenter des résultats préliminaires d'une première opération de terrain réalisée fin 1998, lors de laquelle nous nous sommes attachés à retrouver, le long de la côte, les traces des soulèvements de petite ampleur (quelques centimètres) associés au séisme de 1993, grâce à l'observation et à l'analyse de la croissance des coraux.

2. Observations de terrain

La répartition des coraux dans un récif s'établit de la surface des platiers, juste sous le niveau de la mer, jusqu'à plusieurs dizaines de mètres de profondeur. Seuls les coraux vivant à proximité du niveau de la mer nous intéressent pour l'étude des mouvements les plus récents. En effet, à l'occasion d'une surrection, les organismes qui vivent immédiatement au-dessous du niveau marin se retrouvent totalement ou partiellement émergés, la partie à l'air libre se nécrose, bloquant la croissance verticale de la colonie, alors que la partie encore sous l'eau continue à vivre et à croître latéralement. L'analyse de la morphologie de telles colonies et leur examen par radiographie X (étude sclérochronologique) fournissent des informations sur la direction des axes de croissance et sur les interruptions et reprises de croissance (Knutson et al., 1972 ; Taylor et al., 1982). De telles études ont permis de rendre compte de variations de petite ampleur du niveau marin d'origine tectonique (Taylor et al., 1982 ; Woodroffe et McLean, 1990).

La reconnaissance que nous avons effectuée sur le platier récifal de Vélé, à la pointe sud de l'île de Futuna (*figure 1B*), révèle l'existence d'un ensemble de plusieurs dizaines de constructions coralliennes de *Porites* sp. vivant en limite du niveau marin actuel. Ces colonies, situées sur la partie interne du platier récifal (au sens morphologique du terme), sont régulièrement soumises aux effets de la marée, attestant par là même l'absence de toute retenue d'eau épirécifale. Les colonies ont une morphologie typique de microatolls (*sensu* Stoddart et Scoffin, 1979), liés à des fluctuations récentes du niveau de la mer, en liaison avec des surrections et des submergences (Stoddart et Scoffin, 1979 ; Woodroffe et McLean, 1990). Plusieurs de ces colonies ont été prélevées, puis découpées en tranches de 6 à 7 mm d'épaisseur, afin d'être radiographiées (un exemple est donné sur la *figure 2*). L'examen des radiographies montre des perturbations de la croissance, ainsi que des modifications dans la direction des axes de croissance (*figure 3*). Ainsi, d'après le décompte des bandes de croissance, on observe une croissance qui s'est interrompue aux alentours de 1977, probablement à

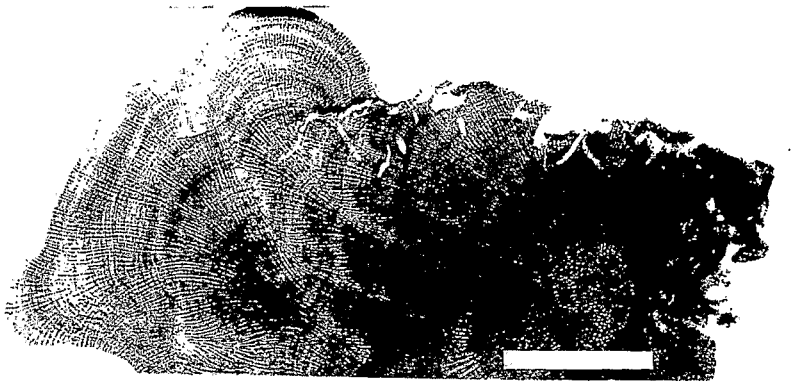

Figure 2. Radiographie X effectuée sur une tranche d'un demi-microatoll de *Porites*, prélevée sur le platier récifal de Vélé. Barre d'échelle = 4 cm.

X-ray radiography obtained from a slab of the half part of a *Porites* microatoll, collected on the Vélé reef flat. Scale = 4 cm.

la suite d'un soulèvement cosismique ; cet événement est marqué par un aplanissement de la surface de la colonie (noté 1 sur la *figure 3*). À compter de cette date, on observe une nouvelle croissance, dont la direction devient peu à peu verticale, ce qui suggère une submergence progressive de la colonie (2). Cette croissance verticale est brutalement interrompue en 1993, comme l'atteste le décompte des bandes, suite à un soulèvement. À partir de 1993, la partie supérieure de la colonie se nécrose et la croissance s'effectue latéralement (3). Cette nécrose semble s'être faite de façon progressive, la partie immédiatement au-dessus du niveau moyen de la mer (à 2 cm environ) ayant cessé de croître immédiatement, alors que la partie au-dessous (à 3 cm environ), a continué à survivre pendant une année ou moins, avant de se nécroser. La hauteur totale nécrosée est donc de 5 cm. Ni apport de sédiments fins, ni recouvrement par des sables, qui pourrait être à l'origine de la nécrose partielle de telles colonies, n'a été observé.

D'autres événements apparaissent à l'examen des radiographies, notamment des perturbations dans la croissance et des densifications des bandes, probablement en liaison avec des événements d'ordre climatique, comme les El Niño. L'interprétation de ces événements est en cours, mais nous nous focaliserons dans cette note sur l'apport de la croissance des coraux à l'étude sismotectonique et, tout particulièrement, à l'analyse de l'événement de 1993.

3. Discussion

L'épicentre du séisme de 1993, déterminé à partir du réseau sismologique mondial, est situé, selon les catalogues disponibles, à une quinzaine de kilomètres à l'ouest (CMTS) ou au sud-ouest (NEIC) de Futuna (*figure 1B*). Cependant, l'installation d'une station sismologique, 2 jours après ce séisme, a permis de localiser une quarantaine de répliques très superficielles juste au sud et sous l'île de Futuna, ce qui suggère que le séisme principal était probablement très superficiel et que sa position réelle était plus à l'est et plus près de d'île de Futuna que celle fournie par le réseau mondial (Régnier, 1994). Cette hypothèse est confirmée par l'amplitude des surrections observées le long de la côte sud de l'île. Si nous prenons la localisation et la solution fournies par le catalogue CMT et si nous estimons la surface de rupture et le glissement, de manière à être en accord avec le moment sismique, les paramètres que nous utilisons sont : épicentre et mécanisme focal CMTS, surface 20 × 10 km, glissement 0,7 m. Les déplacements cosismiques verticaux, calculés avec les modèles

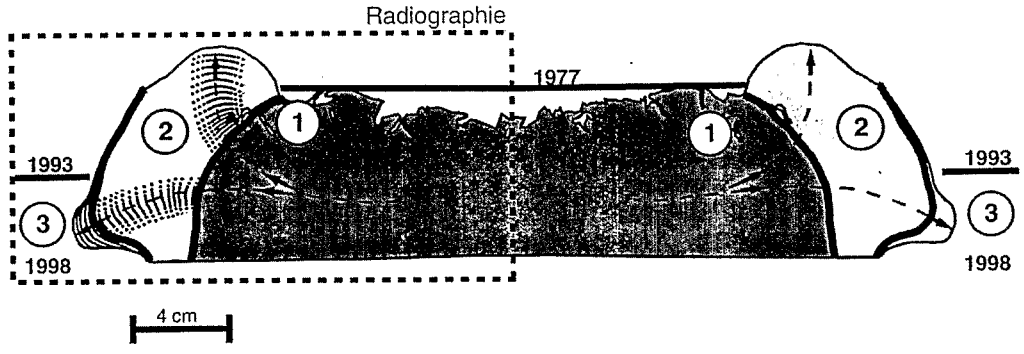

Figure 3. Interprétation de la croissance du microatoll à partir de la radiographie présentée sur la *figure 2*. Les flèches indiquent les directions de croissance, les traits épais les interruptions ou perturbations de croissance liées à des soulèvements cosismiques. Explications des stades 1, 2 et 3 dans le texte.

Interpretation of the microatoll growth by examination of the X-ray radiography shown in *figure 2*. The arrows indicate the growth trends. The thick lines mark the perturbations of the growth related to co-seismic uplifts. Explanation of stages 1, 2 and 3 in the text.

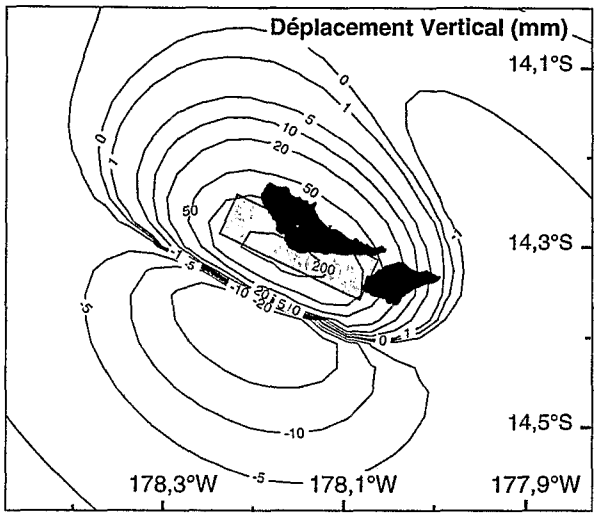

Figure 4. Carte des déplacements verticaux associés au séisme du 12 mars 1993. Ces mouvements ont été modélisés en utilisant le modèle de dislocation d'Okada, avec la solution CMT du séisme, mais en relocalisant la zone de rupture, de manière à obtenir des mouvements verticaux compatibles avec ceux observés le long de la côte sud de l'île de Futuna.

Map of vertical motions related to the 12 March 1993 earthquake. Motions have been modelled applying the dislocation model of Okada to the CMT solution but with a relocated ruptured surface in order to match the vertical motions with the observed uplifts on the reef flats of the south coast of Futuna.

maintenant classiques de Savage (1980) ou Okada (1985), sont minimes et bien inférieurs à ceux observés sur la côte sud de l'île de Futuna. Tout en conservant le moment sismique et le mécanisme au foyer du catalogue CMT, nous avons donc déplacé le centre de la zone de rupture (position et profondeur), afin de rendre compte au mieux des déplacements verticaux observés en surface (*figure 4*). Bien que le nombre des mesures de soulèvement soit très réduit, le domaine de solutions réalistes est assez restreint. Le meilleur ajustement correspond à un événement situé à proximité immédiate de la pointe sud-ouest de Futuna, à 178,15°W et 14,30°S, vers 8 km de profondeur, ce qui engendre un déplacement vertical positif de 20 cm à Léava et de 5 cm à Vélé (*figure 4*). Compte tenu de la très faible profondeur de ce fort séisme (Mw : 6,4, ce qui correspond à une surface de 20 × 10 km pour un glissement de 0,7 m), la rupture a pu quasiment atteindre la surface au sud-ouest de Futuna. Ceci est tout à fait cohérent avec le fait que le séisme a provoqué un raz de marée sur les côtes sud et ouest de l'île. De même, les habitants rapportent avoir entendu le grondement du séisme, ce qui atteste aussi une source superficielle.

Une simulation de l'évolution de la déformation verticale pour le site de Vélé est présentée sur la *figure 5*. Cette simulation est basée sur le modèle de dislocation d'Okada (1985) pour une relaxation de contraintes augmentant

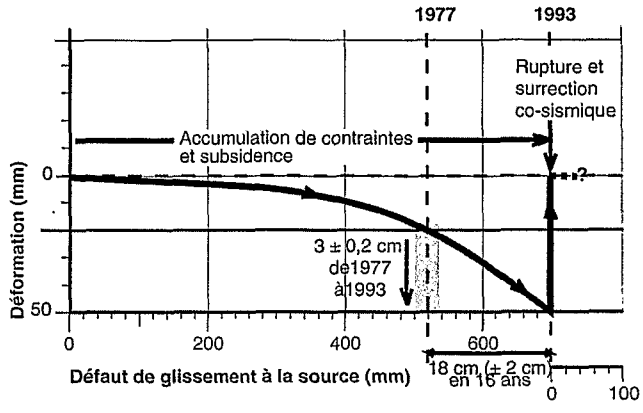

Figure 5. Évolution de la déformation verticale à Vélé, déduite d'une simulation du cycle d'accumulation/relaxation des contraintes associées au séisme du 12 mars 1993 (voir texte) et des observations sur les microatolls.

Evolution of the vertical deformation at Vélé estimated from a simulation of the strain accumulation/relaxation cycle associated to the 12 March 1993 earthquake.

avec le temps, c'est-à-dire pour un glissement de plus en plus grand, sur une faille de plus en plus étendue. Selon ce modèle, les déplacements intersismiques sont égaux et opposés aux mouvements cosismiques et croissent non linéairement avec le temps. La morphologie du corail indique qu'entre 1977 et 1993, le corail a crû verticalement de 3 cm environ (± 2 mm). En considérant que cette mesure correspond à l'ampleur de la subsidence durant cette période, on obtient que le défaut de glissement était de 52 ± 2 cm en 1977 (*figure 5*). La vitesse d'accumulation du défaut de glissement serait alors de (70–52)/(1993–1977) = 1,1 cm·an^{-1} (± 0,2 cm·an^{-1}) et la durée totale de l'accumulation des contraintes jusqu'à rupture sismique aura été de 70/1,1 = 64 ± 12 années. Ces indications sont, à ce jour, données à titre indicatif, car nous ne possédons qu'un nombre limité d'observations de terrain. Cette vitesse constitue toutefois la première estimation, minimale, de la vitesse de convergence au niveau de l'île de Futuna.

4. Conclusion

L'analyse de la croissance des microatolls vivant en limite du niveau marin actuel sur le platier de la côte sud de l'île de Futuna fournit des renseignements précieux sur l'occurrence et l'amplitude des mouvements verticaux récents, et permet d'étudier l'aléa sismique en l'absence de données sismologiques précises. Les mouvements verticaux observés in situ et par radiographie X permettent de préciser la localisation de la faille ayant joué lors du séisme de 1993 et de mettre en évidence l'accumulation des contraintes associées à ce séisme.

Remerciements. Les auteurs remercient vivement pour leur aide, les rois de Sigave et d'Alo, les autorités coutumières et le Délégué du gouvernement ainsi que J.-L. Laurent, F. Afalaato, chef de la Service Météo-France de Futuna, et le Service de radiologie de l'hôpital de Nouméa. Ce travail a bénéficié du soutien financier du PNRN 1998 (Programme national sur les risques naturels). Contribution UHR Géosciences-Azur n° 253.

5. Références

Grzesczyk A., Eissen J.-P., Dupont J., Lefevre C., Maillet P. et Monzier M. 1987. Pétrographie et minéralogie des îles Futuna et Alofi, TOM de Wallis et Futuna (Pacifique sud-ouest), *C. R. Acad. Sci. Paris*, 305, série II, 93–98

Grzesczyk A., Monzier M., Dupont J., Eissen J.-P. et Maillet P. 1989. *Carte géologique à l'échelle 1/25 000e de Futuna et Alofi (îles de Horn)*, TOM de Wallis et Futuna, Orstom Nouméa.

Grzesczyk A., Lefevre C., M. Monzier M., Dupont J., Eissen J.-P. et Maillet P. 1991. Mise en évidence d'un volcanisme transitionnel pliocène supérieur sur Futuna et Alofi (SW Pacifique) : un nouveau témoin de l'évolution géodynamique nord-Tonga, *C. R. Acad. Sci. Paris*, 312, série II, 713–720

Knutson D.W., Buddemeier R.W. et Smith S.V. 1972. Coral chronometers: seasonal growth bands in reef corals, *Science*, 177, 270–272

Louat R., Monzier M., Grzeszyk A., Dupont J., Eissen J.-P. et Maillet P. 1989. Sismicité superficielle à proximité des îles de Horn (Territoire de Wallis et Futuna, Pacifique sud) : caractéristiques et conséquences, *C. R. Acad. Sci. Paris*, 308, série II, 489–494

Monzier M., Régnier M. et Decourt R. 1993. Rapport sur la crise sismique de mars 1993 à Futuna (TOM des îles Wallis et Futuna), *Rapport de missions*, Centre Orstom de Nouméa, 30, 1–23

Okada Y. 1985. Surface displacement due to shear and tensile faults in a half-space, *Bull Seis. Soc. Am.*, 75, 1135–1154

Pelletier B., Calmant S. et Pillet R. 1998. Current tectonics of the Tonga-New Hebrides region, *Earth Planet. Sci. Letters*, 164, 263–276

Régnier M. 1994. Sismotectonique de la ride de Horn (îles de Futuna et Alofi), un segment en compression dans la zone de fracture Nord-Fidjienne, *C. R. Acad. Sci. Paris*, 318, série II, 1219–1224

Savage J. 1980. *In :* Nabarro F.R.N. (éd.), *'Dislocations in seismology' from 'dislocations in solids'*, North Holland Pub. Co., Amsterdam

Stoddart D.R. et Scoffin T.P. 1979. Microatolls: review of form, origin and terminology, *Atoll Research Bull.*, 224, 1–17

Taylor F., Jouannic C., Gilpin L. et Bloom A.L. 1982. Coral colonies as monitors of change in sea level of the land and sea: application to vertical tectonism, *in : Proc. IVth Int. Coral Reef Symp.*, 1, 485–492

Woodroffe C. et McLean R. 1990. Microatolls and recent sea level change on coral atolls, *Nature*, 344, 531–534